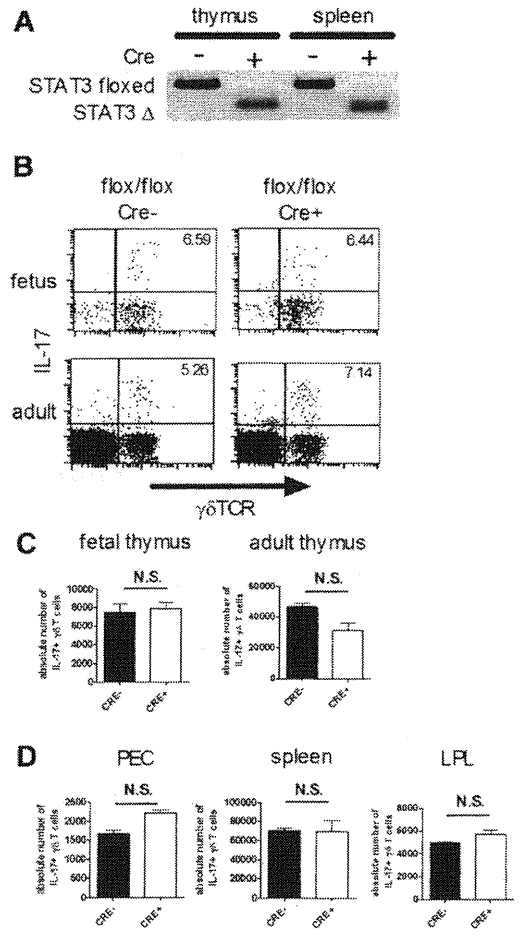

Figure 1. STAT3 is dispensable for the development of IL-17–producing γδ T cells. (A) γδ T-cell–specific disruption of the *STAT3* gene in *STAT3*$^{flox/flox}$ *Tie2-Cre* mice. Genomic DNA was prepared from purified γδ T cells from the thymi and spleens of *STAT3*$^{flox/flox}$ (Cre$^-$) and *STAT3*$^{flox/flox}$ *Tie2-Cre* (Cre$^+$) mice and used for allele-specific PCR analysis. Floxed allele (STAT3 floxed, 350 bp) and disrupted allele (STAT3 Δ, 150 bp) are shown. (B-D) IL-17–producing γδ T cells in *STAT3*$^{flox/flox}$ (Cre$^-$) and *STAT3*$^{flox/flox}$ *Tie2-Cre* (Cre$^+$) mice. Single-cell suspensions of fetal (E16) and adult thymocytes (4 weeks old; B-C) or PEC, spleens, and LPLs (4 weeks old; D) from *STAT3*$^{flox/flox}$ (flox/flox Cre$^-$) and *STAT3*$^{flox/flox}$ *Tie2-Cre* (flox/flox Cre$^+$) mice were stimulated with PMA and ionomycin and analyzed for intracellular staining for IL-17. (B) Representative dot plots of intracellular staining for IL-17 in fetal (top panels) and adult (bottom panels) thymi are shown after gating on CD3$^+$ cells. The number in the top right quadrant indicates the percentage of IL-17$^+$ cells in γδTCR$^+$ cells. (C-D) Absolute numbers of IL-17$^+$ γδ T cells in each organ are shown. Data shown are the means ± SD of 5 mice. N.S. indicates statistically not significant between groups. Data are representative of 3 independent experiments.

absent in the periphery of *RORc*$^{-/-}$ mice (Figure 2C). These results suggest that RORγt is only partly required for intrathymic development of IL-17–producing γδ T cells, but plays indispensable roles in their maintenance in the periphery.

Hes1 expression is correlated with IL-17 production of γδ T cells

To search for the molecule(s) critically involved in the development of IL-17–producing γδ T cells, we established IL-17–producing γδ T-cell hybridoma clones by fusing peritoneal γδ T cells with the AKR thymoma BW5147 (supplemental Figure 3). As the negative control, γδ T-cell hybridoma clones were generated from Vγ5$^+$ γδ T cells in skin IELs (s-IELs), none of which produced IL-17.[11] Comparative gene-expression analysis identified 19 genes that were highly expressed in IL-17$^+$ clones (supplemental Table 1). Among these candidates, we focused on *Hes1*, a member of the family of mammalian bHLH transcriptional repressors, because *Hes1* is highly expressed in fetal thymocytes around E15,[29] when IL-17–producing γδ T cells begin to be detected.[11] We confirmed expression of *Hes1* mRNA selectively in IL-17$^+$ clones by qRT-PCR (Figure 3A). Because Hes5 and Hes1 have redundant functions in neural stem cells,[30] we also analyzed *Hes5* expression in these clones, and it was not detected in either (Figure 3A). The expression level of *RORγt* was not up-regulated in IL-17$^+$ clones (Figure 3A).

We next examined expression of *Hes1* in different subsets of γδ T cells freshly isolated from various organs of normal mice. As shown in Figure 3B, virtually all γδ T cells in the epithelium of female reproductive organs (reproductive IELs [r-IELs]) produced IL-17. Consistent with this, *Hes1* was highly expressed in γδ T cells purified from r-IELs compared with those from s-IELs (Figure 3C). We and others have reported previously that CD25 and CD27 can be used as markers discriminating IL-17- and IFN-γ–producing γδ T cells.[11,31] In the present study, we demonstrated that nearly all CD25$^+$ γδ T cells but not all CD27$^-$ cells in the peritoneal cavity produced IL-17 (Figure 3D). Conversely, the expression level of CD25 on IL-17–producing γδ T cells in the spleen was lower than

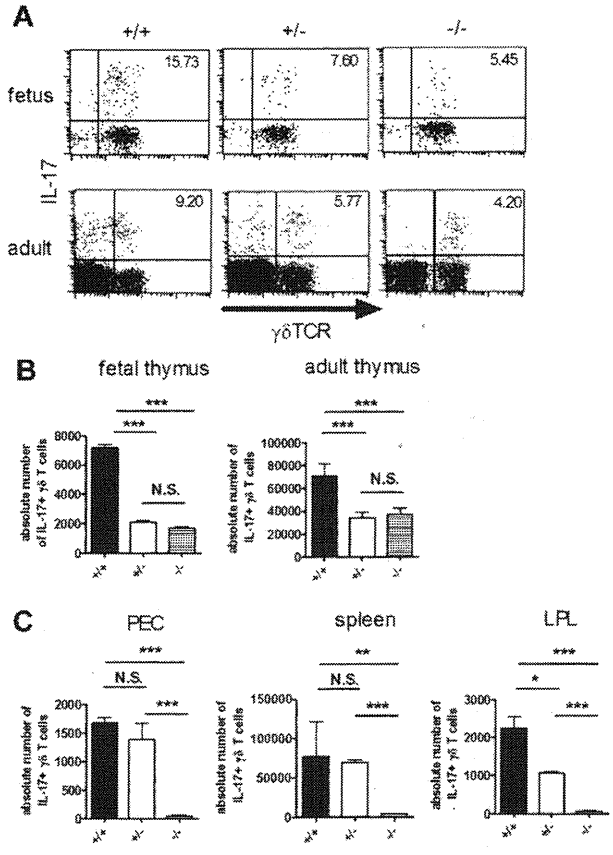

Figure 2. RORγt is partly required for the intrathymic development of IL-17–producing γδ T cells. (A-C) IL-17–producing γδ T cells in *RORc*$^{+/+}$ (+/+), *RORc*$^{+/-}$ (+/−), and *RORc*$^{-/-}$ (−/−) mice. Single-cell suspensions of fetal (E16) and adult thymocytes (6 weeks old; A-B) or PEC, spleen, and LPL (4 weeks old; C) from *RORc*$^{+/+}$ (+/+), *RORc*$^{+/-}$ (+/−), and *RORc*$^{-/-}$ (−/−) mice were stimulated with PMA and ionomycin and analyzed for intracellular staining for IL-17. (A) Representative dot plots of intracellular staining for IL-17 in fetal (top panels) and adult (bottom panels) thymi are shown after gating on CD3$^+$ cells. The number in the top right quadrant indicates the percentage of IL-17$^+$ cells in γδTCR$^+$ cells. (B-C) Absolute numbers of IL-17$^+$ γδ T cells in each organ are shown. Data shown are the means ± SD of 4-5 mice. $^*P < .05$; $^{**}P < .01$; $^{***}P < .001$. N.S. indicates statistically not significant between groups. Data are representative of 3 independent experiments.

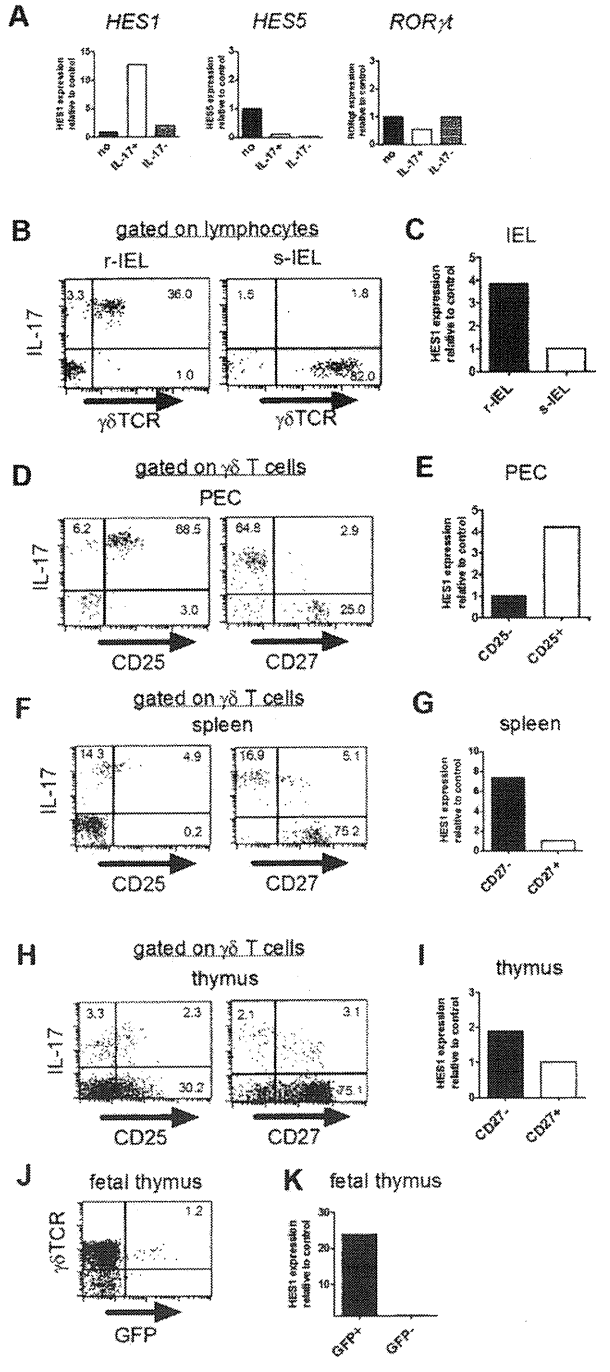

Figure 3. Hes1 is specifically expressed in IL-17–producing γδ T cells. (A) *Hes1* is specifically expressed in IL-17–producing hybridoma clones. (A) mRNA expressions of *Hes1*, *Hes5*, and *RORγt* in parental hybridomas (no), IL-17–producing (IL-17$^+$), and nonproducing (IL-17$^-$) γδ TCR$^+$ hybridoma clones were analyzed by qRT-PCR. (B-K) *Hes1* is specifically expressed in IL-17–producing γδ T cells. (B,D,F,H) Purified γδ T cells from IELs (B), PECs (D), spleens (F), and thymi (8 weeks old; H) were stimulated with PMA and ionomycin and analyzed for intracellular IL-17. Representative dot plots are shown after gating on lymphocytes identified by FSC/SSC profile (B) or γδ TCR$^+$ cells (D,F,H). The numbers in the respective quadrants indicate the percentages of positive cells. (C,E,G,I) Purified γδ T cells from IELs (6 weeks old; C) or sorted CD25^{high}, CD25^{low}, CD27^{high}, and CD27^{low} γδ T cells from PECs (E), spleens (G), and thymi (I) of CβKO mice (6 weeks old) were analyzed for the relative expression of *Hes1*. *Hes1* expression of s-IELs (C), CD25$^-$ γδ T cells (E), or CD27$^+$ γδ T cells (G,I) was set to 1. (J) Fetal thymocytes (E18) of IL-17–GFP reporter mice were analyzed after stimulation with PMA and ionomycin for 4 hours. The number in the top right quadrant indicates the percentage of IL-17$^+$ cells in γδ TCR$^+$ cells. (K) After sorting of GFP$^+$ and GFP$^-$ cells, *Hes1* mRNA expression was analyzed by qRT-PCR. *Hes1* expression of GFP- γδ T cells was set to 1. Data are representative of 3 independent experiments.

that in the PEC, whereas nearly all CD27$^-$ cells in the spleen produced IL-17 (Figure 3F). Based on these findings, we compared the expression of *Hes1* in different subpopulations of γδ T cells in the PEC and spleen, and found that *Hes1* was specifically expressed in CD25$^+$ γδ T cells and CD27$^-$ γδ T cells, respectively (Figure 3E,G). We also examined expression of *Hes1* in thymic γδ T cells. IL-17–producing γδ T cells in adult thymi contains CD27$^+$ cells in addition to CD27$^-$ cells (Figure 3H). Similarly, there were both CD25$^+$ and CD25$^-$ γδ T cells positive for IL-17 in the thymus. Consistent with the expression level of IL-17, *Hes1* expression in CD27$^-$ γδ T cells was slightly higher than that in CD27$^+$ γδ T cells (Figure 3H-I). To more directly examine the relationship between *Hes1* expression and IL-17 production by γδ T cells, we analyzed the fetal thymi of IL-17-GFP reporter mice. After brief stimulation with PMA and ionomycin, some of the γδ T cells became positive for GFP (Figure 3J), which exclusively expressed *Hes1* (Figure 3K). The expression of *Hes1* correlated well with the IL-17–producing function of γδ T cells.

Hes1 is critical for the development of IL-17–producing γδ T cells in the thymus

To determine whether Hes1 is required for the development of IL-17–producing γδ T cells, we analyzed Hes1-deficient mice. Because Hes1-deficient mice die during gestation or just after birth with severe defects of neural tubes and eye morphogenesis,[21] we analyzed fetal thymi on E16 and E18. The absolute number of γδ T cells in the thymi of Hes1-deficient mice was lower than that

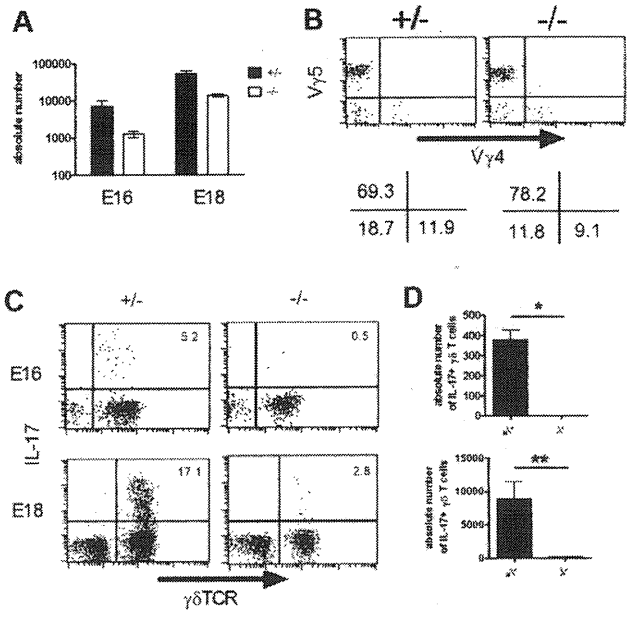

Figure 4. Hes1 is critical for the development of IL-17–producing γδ T cells. (A-B) Hes1 is dispensable for the development of γδ T cells. (A) Absolute numbers of γδ T cells in fetal thymi (E16, left; E18, right) of *Hes1*$^{+/-}$ (+/−) and *Hes1*$^{-/-}$ (−/−) mice were calculated after analyzing by flow cytometry. Data shown are the means ± SD of 4 fetuses for each group. (B) Representative dot plots for the expression of Vγ4 and Vγ5 in fetal thymi (E16) are shown after gating on γδ TCR$^+$ cells. The numbers under each panel indicate the percentages of positive cells in the respective quadrants. (C-D) Hes1 is required for the development of IL-17–producing γδ T cells. IL-17 production by γδ T cells from E16 (top panels) and E18 (bottom panels) of *Hes1*$^{+/-}$ (+/−) and *Hes1*$^{-/-}$ (−/−) mice were analyzed after stimulation with PMA and ionomycin. (C) Representative dot plots are shown after gating on CD3$^+$ cells. The number in the top right quadrant indicates the percentage of IL-17$^+$ cells in γδ TCR$^+$ cells. (D) Absolute numbers of IL-17$^+$ γδ T cells are shown. Data shown are the means ± SD of 4 mice. $^*P < .05$. Data are representative of 3 independent experiments.

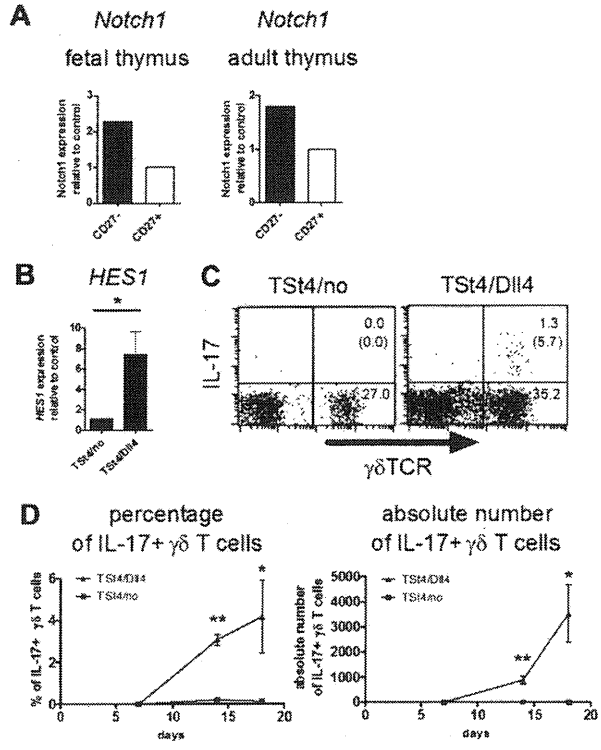

Figure 5. Critical role of Notch-Hes1 pathway for the development of IL-17–producing γδ T cells. (A) *Notch1* expression of γδ T cells in the thymus. Sorted CD27^{high} and CD27^{low} γδ T cells from E18 fetal (left) or adult (right) thymi of CβKO mice (6 weeks old) were analyzed for the relative expression of *Notch1*. *Notch1* expression of CD27$^+$ γδ T cells was set to 1. (B-D) Dll4-mediated Notch signaling induces the development of IL-17–producing γδ T cells. Three thousand fetal thymocytes (E15) were cocultured with TSt-4/no or TSt-4/Dll4 stromal cells. (B) *Hes1* expression was analyzed by qRT-PCR 14 days after the culture. Data shown are the means ± SD of 4 individual wells. *$P < .05$. (C-D) After coculture with TSt-4/no or TSt-4/Dll4 cells, IL-17 production by γδ T cells was analyzed after stimulation with PMA and ionomycin (C). Representative dot plots are shown after gating on CD45.2$^+$ cells. The number in top right or bottom right quadrant indicates γδTCR$^+$IL-17$^+$ or γδTCR$^+$IL-17$^-$ cells in CD45.2$^+$ cells, respectively. The number in the parentheses shows the percentage of IL-17$^+$ cells in γδ TCR$^+$ cells. (D) Kinetics of percentages (left) or absolute numbers (right) of IL-17–producing γδ T cells are shown at the indicated days. Data shown are the means ± SD of 4 individual wells at each time point. *$P < .05$; **$P < .01$. Data are representative of 3 independent experiments.

of control mice (Figure 4A), which is consistent with a previous report in which Hes1 was shown to play an important role in the expansion of early T-cell precursors.[29] All γδ T-cell repertoires developed normally in the absence of Hes1 (Figure 4B); however, IL-17–producing γδ T cells were strikingly decreased in Hes1-deficient mice (Figure 4C-D), indicating that Hes1 plays a critical role in the development of IL-17–producing γδ T cells in fetal thymi.

Notch-Hes1 pathway is involved in the development of IL-17–producing γδ T cells

Hes1 is known as a downstream signaling molecule of Notch receptors, such as Notch1, Notch2, Notch3, and Notch4.[32] It was shown previously that *Notch1* expression was detected on fetal thymic γδ T cells on E16.[33] Consistent with *Hes1* expression (Figure 3I and data not shown), CD27$^-$ γδ T cells expressed a relatively higher level of *Notch1* than CD27$^+$ γδ T cells in the fetal and adult thymus (Figure 5A). It is of interest to examine the role of Notch and its ligands, including Dll1, Dll3, Dll4, and Jagged 1 and 2, in the development of IL-17–producing γδ T cells in the thymus. However, Notch signaling, especially the Notch1-Dll4 interaction, is indispensable for early T-cell development in the thymus.[34,35] In addition, mice deficient for Notch1 or Dll4 are embryonically lethal.[36,37] Therefore, we analyzed the involvement of Dll4-mediated Notch signaling in γδ T-cell differentiation in vitro using TSt4 stromal cells. In addition to CD4$^+$CD8$^+$ double-positive cells, γδ T cells, some of which produced IL-17, developed from hematopoietic progenitor cells in the fetal liver after culture with TSt4/Dll4 cells (data not shown). However, consistent with the previous report,[24] only NK and B cells, but not T cells, developed in the absence of Notch signaling. Therefore, it was impossible to separately analyze the development and function of γδ T cells in this system. To circumvent this problem, we cultured fetal thymocytes (E15), in which T-cell–committed progenitors had already developed, with the stromal cells. In this system, γδ T cells developed even in the absence of Notch signaling (Figure 5C). However, the expression level of *Hes1* in γδ T cells was greatly diminished in the absence of Notch signaling, indicating the importance of Notch signaling in *Hes1* expression (Figure 5B). Furthermore, the development of IL-17–producing γδ T cells was not detected in the culture without Notch signaling (Figure 5C-D).

To further confirm the importance of Notch-Hes1 pathway in the development of IL-17–producing γδ T cells in vivo, fetal liver cells were introduced with intracellular Notch1 (ICN1), which activates Notch signaling by bypassing Notch-Notch ligand interaction. The ICN1-transduced cells were transferred into irradiated recipient mice, which were analyzed after 4 weeks. Constitutively active Notch signaling augmented *Hes1* expression in thymocytes (supplemental Figure 4A). Consistent with a previous report,[34] an increased percentage of CD4$^+$CD8$^+$ double-positive cells in the thymus was observed (supplemental Figure 4B). It was also found that introducing ICN1 greatly increased the percentage of IL-17–producing γδ T cells (supplemental Figure 4C-D). Therefore, the Notch-Hes1 pathway is critical for the development of naturally occurring IL-17–producing γδ T cells in the thymus.

Importance of Hes1 in mature IL-17–producing γδ T cells in the periphery

Notch1 as well as *Hes1* was expressed in IL-17–producing (CD27$^-$) γδ T cells in the periphery, suggesting the involvement of the Notch-Hes1 pathway at this stage (Figures 3G and 6B). Therefore, we generated conditional Hes1-deficient mice by crossing *Hes1*$^{flox/flox}$ mice with *MX1-Cre* Tg mice, in which the *Hes1* gene was deleted by poly I:C injection. Vγ4$^+$ γδ T cells are known to be part of the major repertoire of IL-17–producing γδ T cells in the periphery.[38] In fact, IL-17–producing Vγ4$^+$ γδ T cells were abundantly found in the thymus as well as in the periphery of adult mice (Figure 6A). Because *Hes1* expression was efficiently eliminated in γδ T cells in the spleen but not in the thymus after poly I:C injection (supplemental Figure 5), splenic IL-17–producing γδ T cells were analyzed. We found that IL-17 production by γδ T cells was significantly reduced in the absence of Hes1 (Figure 6C-E). The significant decrease of the percentage of IL-17–producing cells was detected within CD27$^-$ γδ T cells (Figure 6D). The number of IFN-γ–producing γδ T cells was not reduced by *Hes1* ablation (Figure 6C,E). The number of IL-17–producing γδ TCR$^-$ splenocytes, most of which were CD4$^+$ αβ T cells, was also unaffected by the absence of Hes1 (supplemental Figure 6, data not shown). These results suggest that Hes1 is selectively involved in the IL-17–producing function of mature γδ T cells in the periphery.

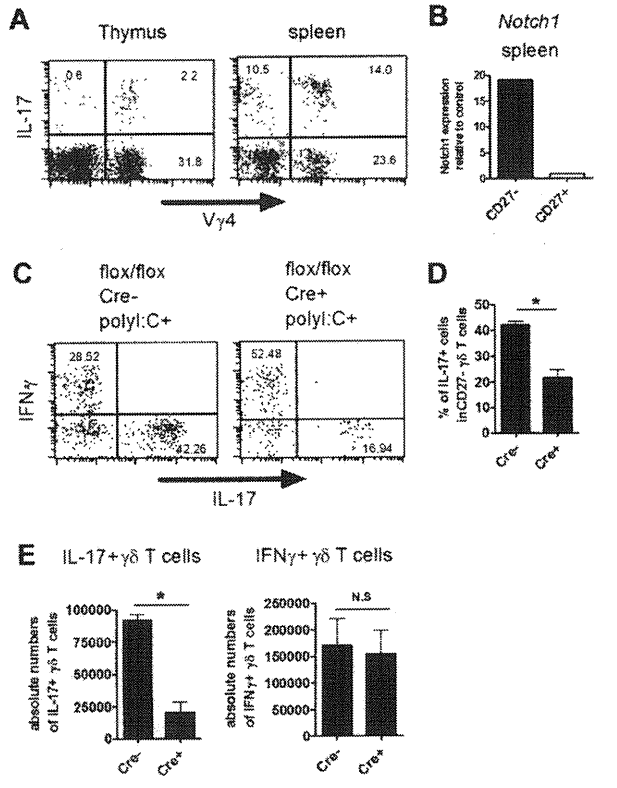

Figure 6. Important role of Hes1 in IL-17–producing γδ T cells in the periphery. (A) Vγ4$^+$ IL-17–producing γδ T cells in the thymi and spleens of adult mice. Single-cell suspensions of thymocytes and splenocytes from adult mice (6 weeks old) were stimulated with PMA and ionomycin and analyzed for IL-17–producing cells. Representative dot plots are shown after gating on γδ TCR$^+$ cells. (B) Sorted Vγ4$^+$ CD27^{high} and CD27^{low} γδ T cells from spleens were analyzed for the relative expression of *Notch1*. *Notch1* expression of CD27$^+$ γδ T cells was set to 1. (C-E) Hes1 is selectively involved in IL-17 production by γδ T cells in the periphery. Splenocytes from *HES1*$^{flox/flox}$ (flox/flox Cre$^-$) and *HES1*$^{flox/flox}$ *MX1-Cre* (flox/flox Cre$^+$) mice (4 weeks old) were prepared 4 days after the last poly I:C injection. (C-D) IFN-γ and IL-17 production by Vγ4$^+$ γδ T cells was analyzed after stimulation with PMA and ionomycin. (C) Representative dot plots are shown after gating on Vγ4$^+$ γδ T cells. The numbers in the respective quadrants indicate the percentage of cells. (D) Percentage of IL-17$^+$ cells within CD27$^-$ Vγ4$^+$ γδ T cells are shown. Data shown are the means ± SD of 3 mice. (E) Absolute numbers of IFN-γ- or IL-17–producing Vγ4$^+$ γδ T cells are shown. Data shown are the means ± SD of 5 mice. *$P < .05$. N.S. indicates statistically not significant between groups. Data are representative of 3 independent experiments.

Discussion

The acquisition of effector T-cell functions is regulated by various cell-intrinsic and cell-extrinsic factors. STAT3 and RORγt are required for the differentiation of Th17- and IL-17–producing NKT cells. In the present study, we found that Hes1, a bHLH protein induced by Notch signaling, is critically involved in the development of naturally occurring IL-17–producing γδ T cells, which develop profoundly in the perinatal thymus.

In Th17 cells, STAT3 plays an important role in transducing IL-6 receptor signaling. Consistent with our finding that IL-17–producing γδ T cells developed in STAT3-deficient mice, it was reported that IL-6 was required for the differentiation of IL-17–producing αβ T cells, but not for γδ T cells.[16] Interestingly, IL-17–producing NKT cells develop normally in IL-6–deficient mice,[14] suggesting that the development of IL-17–producing γδ T cells and NKT cells is regulated by a similar mechanism. However, whereas intrathymic development of IL-17–producing γδ T cells is partly dependent on RORγt, that of IL-17–producing NKT cells requires *RORγt* expression.[15] RORγt-independent development of IL-17–producing γδ T cells is supported by our previous finding that *RORγt* expression was detected in the CD25$^-$CD122$^+$ population of γδ T cells, which only produce IFN-γ.[11] In addition, a study using RORγt reporter mice demonstrated expression of RORγt in Vγ5$^+$ γδ T cells in the skin, which do not produce IL-17.[16] Therefore, the expression level of RORγt is not necessarily related to IL-17 production in γδ T cells. Interestingly, IL-17–producing γδ T cells were absent in the periphery of RORγt-deficient mice, suggesting the importance of RORγt at this stage. In agreement with this, Ribot et al observed increased expression of RORγt in IL-17–producing CD27$^-$ γδ T cells in the periphery.[31] RORγt was initially identified as a molecule that is highly expressed in double-positive thymocytes and promotes their survival by up-regulating the expression of Bcl-xL.[20] It has yet to be determined whether RORγt plays a similar antiapoptotic role in IL-17–producing γδ T cells in the periphery. A small number of Th17 cells naturally develop in STAT3-deficient and RORγt-deficient mice,[25,28] suggesting that some αβ T cells share a differentiation mechanism with γδ T cells.

Hes1 is known to regulate the fate of various cell lineages in developing organs, including T cells.[39] It was shown previously that Hes1-deficient fetal liver cells had a severe defect in reconstituting T cells in Rag1-deficient mice.[29] Fetal thymic organ culture revealed that the cellularity was significantly reduced in Hes1-deficient thymic lobes.[40] Hes1 overexpression in T cells potentially induces T-cell lymphoma.[41,42] In addition, Hes1 promotes the commitment of αβ T cells toward the CD8 lineage by repressing expression of the CD4 receptor.[43] In the present study, we identified a novel role of Hes1 in developing T cells. Hes1 is involved in the development of IL-17–producing γδ T cells in the thymus. At present, the molecular mechanisms through which Hes1 induces the development of IL-17–producing γδ T cells is unclear. Hes1 is known to promote or inhibit cell-cycle progression by regulating the expression of cell-cycle regulators such as p27^{Kip1} or E2F-1, respectively, depending on the level of *Hes1* expression.[44,45] Indeed, the number of γδ T cells in the fetal thymi of Hes1-deficient mice was slightly decreased (Figure 4A). Although there was no significant bias in the TCR repertoire, Hes1 might promote the expansion of the IL-17–producing γδ T-cell population. Because Hes1 is known as a transcriptional repressor, it seems unlikely that Hes1 directly induces IL-17 production by binding to regulatory regions of the *IL-17* gene. Nevertheless, recent studies have demonstrated an involvement of Notch signaling in the regulation of IL-17 production by Th17 cells in vitro and in vivo.[46,47] Direct interaction of RBPjκ (also known as CSL), a DNA-binding protein downstream of Notch signaling, with the *IL17* promoter was also shown.[47]

We found here that inactivation of the *Hes1* gene in peripheral γδ T cells selectively reduced IL-17 production, which is consistent with the expression of *Hes1* in IL-17–producing γδ T cells. Furthermore, Dll4 expression was detected in peripheral tissues such as the intestine and lung, where IL-17–producing γδ T cells are abundantly found.[48] These findings imply that Notch receptors continuously transmit signals to maintain *Hes1* expression in IL-17–producing γδ T cells in the periphery. It is possible that Hes1 promotes the survival of IL-17–producing γδ T cells in the periphery. Alternatively, Hes1 may be directly involved in IL-17 production of γδ T cells, as discussed in the preceding paragraph; further studies are required to clarify the molecular mechanisms. In contrast to γδ T cells, the number of peripheral IL-17–producing αβ T cells, most of which were CD4$^+$, was not reduced by

conditional deletion of *Hes1*, indicating lineage-specific roles of Hes1. Although we detected a few IL-17$^+$ CD4$^+$ αβ T cells in adult but not in fetal thymi, it is unclear whether their development is also independent of Hes1, because Hes1-deficient mice do not live longer than the perinatal period and the *Hes1* gene in adult thymocytes was not efficiently deleted in the conditional knockout mice (supplemental Figure 5).

Notch signaling is well known for its role in the development of αβ T cells, but it is also required for the development of γδ T cells.[34,35] Notch signaling is also known to regulate the differentiation of helper CD4$^+$ αβ T cells, although the requirement for Notch signaling is not always absolute in this case.[32] The results of the present study revealed that Notch signaling is involved in and even indispensable for the development of IL-17–producing γδ T cells. IFNγ-producing γδ T cells, which are also known to be generated in the thymus, were infrequently detected in our system (data not shown). It has been suggested that additional signals, including TCR- and/or CD27-mediated signals, are required for the functional differentiation of IFNγ-producing γδ T cells.[31,49] Although our results clearly reveal the importance of Hes1 in developing γδ T cells, the induction of Hes1 does not account for all of the effects of Notch signaling in γδ T cells. The reduced but significant number of γδ T cells in the thymi of *Hes1*-deficient mice revealed the Hes1-independent mechanism of Notch signaling in the development of γδ T cells. Because accumulating evidence indicates the importance of IL-17–producing γδ T cells in vivo,[9,10] our results shed light on novel roles of the Notch-Notch ligand system in the regulation of immune responses.

Acknowledgments

The authors thank Kiyomi Akasaki and Akiko Yano for secretarial assistance, Takanori Nakamura and Amago Michi for microarray analysis, and Toshio Kitamura for providing packaging cell lines and vectors for retroviral transduction.

This work was supported by a Grant-in-Aid for Scientific Research from the Japan Society for Promotion of Science, by The Mochida Memorial Foundation for Medical and Pharmaceutical Research, and by the program of Founding Research Centers for Emerging and Reemerging Infectious Diseases launched as a project commissioned by the Ministry of Education, Culture, Sports, Science and Technology (MEXT) of Japan.

Authorship

Contribution: K.S. and H.Y. designed the research; K.S., T.D., M.N., T.S., and H.T. performed experiments and analyzed data; R.K., Y.I., H.H., S.Y., T.I., and H.K. provided essential materials and protocols; Y.Y. supervised the experimental work; and K.S. and H.Y. wrote the manuscript.

Conflict-of-interest disclosure: The authors declare no competing financial interests.

Correspondence: Kensuke Shibata or Hisakata Yamada, Division of Host Defense, Medical Institute of Bioregulation, Kyushu University, 3-1-1, Maidashi, Higashi-ku, Fukuoka, Japan; e-mail: k_shibata@bioreg.kyushu-u.ac.jp or hisakata@bioreg.kyushu-u. ac.jp.

References

1. Yang XO, Pappu BP, Nurieva R, et al. T helper 17 lineage differentiation is programmed by orphan nuclear receptors ROR alpha and ROR gamma. *Immunity.* 2008;28(1):29-39.
2. Ichiyama K, Yoshida H, Wakabayashi Y, et al. Foxp3 inhibits RORgammat-mediated IL-17A mRNA transcription through direct interaction with RORgammat. *J Biol Chem.* 2008;283(25):17003-17008.
3. Wei L, Laurence A, Elias KM, O'Shea JJ. IL-21 is produced by Th17 cells and drives IL-17 production in a STAT3-dependent manner. *J Biol Chem.* 2007;282(48):34605-34610.
4. Zhou L, Lopes JE, Chong MM, et al. TGF-beta-induced Foxp3 inhibits T(H)17 cell differentiation by antagonizing RORgammat function. *Nature.* 2008;453(7192):236-240.
5. Riol-Blanco L, Lazarevic V, Awasthi A, et al. IL-23 receptor regulates unconventional IL-17-producing T cells that control bacterial infections. *J Immunol.* 2010;184(4):1710-1720.
6. Michel ML, Keller AC, Paget C, et al. Identification of an IL-17-producing NK1.1(neg) iNKT cell population involved in airway neutrophilia. *J Exp Med.* 2007;204(5):995-1001.
7. Stark MA, Huo Y, Burcin TL, et al. Phagocytosis of apoptotic neutrophils regulates granulopoiesis via IL-23 and IL-17. *Immunity.* 2005;22(3):285-294.
8. Tajima M, Wakita D, Noguchi D, et al. IL-6-dependent spontaneous proliferation is required for the induction of colitogenic IL-17-producing CD8+ T cells. *J Exp Med.* 2008;205(5):1019-1027.
9. Matsuzaki G,Umemura M. Interleukin-17 as an effector molecule of innate and acquired immunity against infections. *Microbiol Immunol.* 2007; 51(12):1139-1147.
10. Bonneville M, O'Brien RL,Born WK. Gammadelta T cell effector functions: a blend of innate programming and acquired plasticity. *Nat Rev Immunol.* 2010;10(7):467-478.
11. Shibata K, Yamada H, Nakamura R, et al. Identification of CD25 + gamma delta T cells as fetal thymus-derived naturally occurring IL-17 producers. *J Immunol.* 2008;181(9):5940-5947.
12. Bendelac A, Bonneville M, Kearney JF. Autoreactivity by design: innate B and T lymphocytes. *Nat Rev Immunol.* 2001;1(3):177-186.
13. Benlagha K, Kyin T, Beavis A, Teyton L, Bendelac A. A thymic precursor to the NK T cell lineage. *Science.* 2002;296(5567):553-555.
14. Rachitskaya AV, Hansen AM, Horai R, et al. Cutting edge: NKT cells constitutively express IL-23 receptor and RORgammat and rapidly produce IL-17 upon receptor ligation in an IL-6-independent fashion. *J Immunol.* 2008;180(8):5167-5171.
15. Michel ML, Mendes-da-Cruz D, Keller AC, et al. Critical role of ROR-gammat in a new thymic pathway leading to IL-17-producing invariant NKT cell differentiation. *Proc Natl Acad Sci U S A.* 2008;105(50):19845-19850.
16. Lochner M, Peduto L, Cherrier M, et al. In vivo equilibrium of proinflammatory IL-17 + and regulatory IL-10 + Foxp3 + RORgamma t + T cells. *J Exp Med.* 2008;205(6):1381-1393.
17. Do JS, Fink PJ, Li L, et al. Cutting edge: spontaneous development of IL-17-producing gamma delta T cells in the thymus occurs via a TGF-beta 1-dependent mechanism. *J Immunol.* 2010; 184(4):1675-1679.
18. Takeda K, Kaisho T, Yoshida N, et al. Stat3 activation is responsible for IL-6-dependent T cell proliferation through preventing apoptosis: generation and characterization of T cell-specific Stat3-deficient mice. *J Immunol.* 1998;161(9): 4652-4660.
19. Kisanuki YY, Hammer RE, Miyazaki J, et al. Tie2-Cre transgenic mice: a new model for endothelial cell-lineage analysis in vivo. *Dev Biol.* 2001; 230(2):230-242.
20. Sun Z, Unutmaz D, Zou YR, et al. Requirement for RORgamma in thymocyte survival and lymphoid organ development. *Science.* 2000; 288(5475):2369-2373.
21. Ishibashi M, Ang SL, Shiota K, et al. Targeted disruption of mammalian hairy and Enhancer of split homolog-1 (HES-1) leads to up-regulation of neural helix-loop-helix factors, premature neurogenesis, and severe neural tube defects. *Genes Dev.* 1995;9(24):3136-3148.
22. Imayoshi I, Shimogori T, Ohtsuka T, Kageyama R. Hes genes and neurogenin regulate non-neural versus neural fate specification in the dorsal telencephalic midline. *Development.* 2008;135(15): 2531-2541.
23. Sano S, Itami S, Takeda K, et al. Keratinocyte-specific ablation of Stat3 exhibits impaired skin remodeling, but does not affect skin morphogenesis. *EMBO J.* 1999;18(17):4657-4668.
24. Ikawa T, Hirose S, Masuda K, et al. An essential developmental checkpoint for production of the T cell lineage. *Science.* 2010;329(5987):93-96.
25. Harris TJ, Grosso JF, Yen HR, et al. Cutting edge: An in vivo requirement for STAT3 signaling in TH17 development and TH17-dependent autoimmunity. *J Immunol.* 2007;179(7):4313-4317.
26. Takeda K, Noguchi K, Shi W, et al. Targeted disruption of the mouse Stat3 gene leads to early embryonic lethality. *Proc Natl Acad Sci U S A.* 1997;94(8):3801-3804.
27. Takakura N, Huang XL, Naruse T, et al. Critical role of the TIE2 endothelial cell receptor in the development of definitive hematopoiesis. *Immunity.* 1998;9(5):677-686.
28. Ivanov II, McKenzie BS, Zhou L, et al. The orphan

nuclear receptor RORgammat directs the differentiation program of proinflammatory IL-17+ T helper cells. *Cell.* 2006;126(6):1121-1133.

29. Tomita K, Hattori M, Nakamura E, et al. The bHLH gene Hes1 is essential for expansion of early T cell precursors. *Genes Dev.* 1999;13(9): 1203-1210.
30. Ohtsuka T, Sakamoto M, Guillemot F, Kageyama R. Roles of the basic helix-loop-helix genes Hes1 and Hes5 in expansion of neural stem cells of the developing brain. *J Biol Chem.* 2001;276(32): 30467-30474.
31. Ribot JC, deBarros A, Pang DJ, et al. CD27 is a thymic determinant of the balance between interferon-gamma- and interleukin 17-producing gammadelta T cell subsets. *Nat Immunol.* 2009;10(4): 427-436.
32. Radtke F, Fasnacht N, Macdonald HR. Notch signaling in the immune system. *Immunity.* 2010; 32(1):14-27.
33. Fiorini E, Merck E, Wilson A, et al. Dynamic regulation of notch 1 and notch 2 surface expression during T cell development and activation revealed by novel monoclonal antibodies. *J Immunol.* 2009;183(11):7212-7222.
34. Hozumi K, Mailhos C, Negishi N, et al. Delta-like 4 is indispensable in thymic environment specific for T cell development. *J Exp Med.* 2008;205(11): 2507-2513.
35. Radtke F, Wilson A, Stark G, et al. Deficient T cell fate specification in mice with an induced inactivation of Notch1. *Immunity.* 1999;10(5):547-558.
36. Swiatek PJ, Lindsell CE, del Amo FF, Weinmaster G, Gridley T. Notch1 is essential for postimplantation development in mice. *Genes Dev.* 1994;8(6):707-719.
37. Krebs LT, Shutter JR, Tanigaki K, et al. Haploinsufficient lethality and formation of arteriovenous malformations in Notch pathway mutants. *Genes Dev.* 2004;18(20):2469-2473.
38. Roark CL, French JD, Taylor MA, et al. Exacerbation of collagen-induced arthritis by oligoclonal, IL-17-producing gamma delta T cells. *J Immunol.* 2007;179(8):5576-5583.
39. Kageyama R, Ohtsuka T, Kobayashi T. The Hes gene family: repressors and oscillators that orchestrate embryogenesis. *Development.* 2007; 134(7):1243-1251.
40. Kaneta M, Osawa M, Sudo K, et al. A role for pref-1 and HES-1 in thymocyte development. *J Immunol.* 2000;164(1):256-264.
41. Wendorff AA, Koch U, Wunderlich FT, et al. Hes1 is a critical but context-dependent mediator of canonical Notch signaling in lymphocyte development and transformation. *Immunity.* 2010;33(5): 671-684.
42. Dudley DD, Wang HC, Sun XH. Hes1 potentiates T cell lymphomagenesis by up-regulating a subset of notch target genes. *PLoS ONE.* 2009;4(8): e6678.
43. Allen RD 3rd, Kim HK, Sarafova SD, Siu G. Negative regulation of CD4 gene expression by a HES-1-c-Myb complex. *Mol Cell Biol.* 2001;21(9): 3071-3082.
44. Hartman J, Muller P, Foster JS, et al. HES-1 inhibits 17beta-estradiol and heregulin-beta1-mediated upregulation of E2F-1. *Oncogene.* 2004;23(54):8826-8833.
45. Murata K, Hattori M, Hirai N, et al. Hes1 directly controls cell proliferation through the transcriptional repression of p27Kip1. *Mol Cell Biol.* 2005; 25(10):4262-4271.
46. Ito T, Schaller M, Hogaboam CM, et al. TLR9 regulates the mycobacteria-elicited pulmonary granulomatous immune response in mice through DC-derived Notch ligand delta-like 4. *J Clin Invest.* 2009;119(1):33-46.
47. Mukherjee S, Schaller MA, Neupane R, Kunkel SL, Lukacs NW. Regulation of T cell activation by Notch ligand, DLL4, promotes IL-17 production and Rorc activation. *J Immunol.* 2009;182(12):7381-7388.
48. Benedito R, Duarte A. Expression of Dll4 during mouse embryogenesis suggests multiple developmental roles. *Gene Expr Patterns.* 2005;5(6): 750-755.
49. Jensen KD, Su X, Shin S, et al. Thymic selection determines gammadelta T cell effector fate: antigen-naive cells make interleukin-17 and antigen-experienced cells make interferon gamma. *Immunity.* 2008;29(1):90-100.

THE JOURNAL OF BIOLOGICAL CHEMISTRY VOL. 286, NO. 19, pp. 16800–16806, May 13, 2011

A Microbial Glycolipid Functions as a New Class of Target Antigen for Delayed-type Hypersensitivity*

Received for publication, December 28, 2010, and in revised form, March 24, 2011 Published, JBC Papers in Press, March 25, 2011, DOI 10.1074/jbc.M110.217224

Takaya Komori[‡§], Takashi Nakamura[¶], Isamu Matsunaga[‡§], Daisuke Morita[‡§], Yuki Hattori[‡§], Hirotaka Kuwata[‡], Nagatoshi Fujiwara[‖], Kenji Hiromatsu[**], Hideyoshi Harashima[¶], and Masahiko Sugita[‡§1]

From the [‡]Laboratory of Cell Regulation, Institute for Virus Research, Kyoto University, Kyoto 606-8507, Japan, the [§]Laboratory of Cell Regulation and Molecular Network, Graduate School of Biostudies, Kyoto 606-8507, Japan, [¶]Faculty of Pharmaceutical Sciences, Hokkaido University, Sapporo 060-0812, Japan, the [‖]Department of Bacteriology, Osaka City University Graduate School of Medicine, Osaka 545-8585, Japan, and the [**]Department of Microbiology and Immunology, Faculty of Medicine, Fukuoka University, Fukuoka 814-0180, Japan

Delayed-type hypersensitivity (DTH) is marked by high levels of protein antigen-specific T cell responses in sensitized individuals. Recent evidence has revealed a distinct pathway for T cell immunity directed against glycolipid antigens, but DTH to this class of antigen has been undetermined and difficult to prove due to their insolubility in aqueous solutions. Here, glucose monomycolate (GMM), a highly hydrophobic glycolipid of the cell wall of mycobacteria, was dispersed in aqueous solutions in the form of octaarginine-modified liposomes and tested for its ability to elicit cutaneous DTH responses in bacillus Calmette-Guerin (BCG)-immunized guinea pigs. After an intradermal challenge with the GMM liposome, a significant skin induration was observed in BCG-immunized, but not mock-treated, animals. The skin reaction peaked at around 2 days with local infiltration by mononuclear cells, and therefore, the response shared basic features with the classical DTH to protein antigens. Lymph node T cells from BCG-immunized guinea pigs specifically increased IFN-γ transcription in response to the GMM liposome, and this response was completely blocked by antibodies to CD1 lipid antigen-presenting molecules. Finally, whereas the T cells increased transcription of both T helper (Th) 1-type (IFN-γ and TNF-α) and Th2-type (IL-5 and IL-10) cytokines in response to the purified protein derivative or tuberculin, their GMM-specific response was skewed to Th1-type cytokine production known to be critical for protection against tuberculosis. Thus, our study reveals a novel form of DTH with medical implications.

Delayed-type hypersensitivity (DTH)[2] is marked by high levels of memory T cell immunity directed against protein antigens (Ags). Unlike the immediate-type hypersensitivity that occurs within minutes of an Ag challenge and is associated with specific antibody responses, DTH begins to manifest several hours after an Ag challenge with the peak response reached at around 2 days and primarily involves cell-mediated immunity. The DTH response is readily elicited by an intradermal challenge with the mycobacteria-derived purified protein derivative (PPD) in sensitized individuals, such as those either infected with *Mycobacterium tuberculosis*, the microorganism causing tuberculosis, or vaccinated with bacillus Calmette-Guerin (BCG), an attenuated vaccine strain of *Mycobacterium bovis* (1, 2). Therefore, the tuberculin skin test is of medical importance not only for the diagnosis of mycobacterial infections but also for evaluation of the status of cell-mediated immunity.

Besides protein Ags, presented to T cells by MHC-encoded molecules, the list of Ags recognized by T cells has recently been expanded to include glycolipid Ags, which are presented by non-MHC-encoded molecules of the group 1 CD1 family (3–5). Human group 1 CD1 molecules (CD1a, CD1b, and CD1c) are expressed prominently in activated macrophages and dendritic cells, the two major target cell types for mycobacterial infection, and their role in eliciting T cell immunity against tuberculosis has been noted (6, 7). Furthermore, vaccination with *M. tuberculosis*-derived lipids and glycolipids confers protective immunity in the guinea pig model of human tuberculosis, implying pathways for host defense that are distinct from those directed against protein Ags (8). Despite advances in our understanding of the group 1 CD1-dependent T cell response to mycobacteria-derived glycolipid Ags, DTH responses to this chemical class of Ags have not been fully assessed. Because of the distinct pathways for host responses to protein and glycolipid Ags, the hypersensitivity response to glycolipids would be substantially different from that directed against proteins.

Previously, we detected skin hypersensitivity responses in sensitized guinea pigs, which were directed toward trehalose dimycolate (TDM), one of the major surface-exposed mycolylglycolipids expressed in the cell wall of mycobacteria (9). Although it peaked around 2 days after the challenge, the TDM-elicited response was marked by local infiltration by eosinophils rather than mononuclear cells, and therefore, the response was of a type distinct from that classically defined as DTH. Subsequent biochemical and enzymatic studies revealed that mycobacteria-derived mycolyltransferases, a family of enzymes catalyzing the final step of TDM biosynthesis, could mediate

* This work was supported by grants from the Ministry of Education, Culture, Sports, Science, and Technology (grant-in-aid for Scientific Research on Priority Areas) and from the Japan Society for the Promotion of Science (grant-in-aid for Scientific Research (B) (to M. S.)).

[1] To whom correspondence should be addressed: 53-Kawahara-cho, Shogoin, Sakyo-ku, Kyoto 606-8507, Japan. Tel.: 81-75-751-4028; Fax: 81-75-752-3232; E-mail address: msugita@virus.kyoto-u.ac.jp.

[2] The abbreviations used are: DTH, delayed-type hypersensitivity; BCG, bacillus Calmette-Guerin; C/M, chloroform/methanol; GMM, glucose monomycolate; PPD, purified protein derivative; TCR, T cell receptor; TDM, trehalose dimycolate; Th, T helper; Ag, antigen.

up-regulated production of glucose monomycolate (GMM) when the microbes entered into a host where glucose was readily available as a substrate (10). This observation as well as the fact that GMM is a well-defined glycolipid Ag presented by human CD1b molecules (11, 12) prompted us to test for GMM-elicited DTH responses. By using octaarginine-modified liposomes that contain mycobacteria-derived highly hydrophobic GMM molecules, the present study found that GMM induces DTH responses that are comparable with the classically defined DTH to proteins. These results indicate that a microbial glycolipid functions as a new chemical class of Ag targeted by DTH reactions. In addition, unlike the hypersensitivity to PPD, the GMM-elicited DTH is highly skewed toward T helper (Th) 1-type cytokine production, suggesting a role in host immunity against infections by intracellular microbes, such as *M. tuberculosis*.

EXPERIMENTAL PROCEDURES

Purification of GMM—Chemical reagents were purchased from Nacalai Tesque (Kyoto, Japan) unless otherwise indicated. *Mycobacterium avium* (serovar 4) was kindly provided by Dr. Ikuya Yano (Japan BCG Laboratory, Tokyo, Japan) and grown at 37 °C in 7H9 medium supplemented with the Middlebrook ADC enrichment (BD Biosciences), 5% glucose, and 0.05% Tween 80. The bacteria were harvested when the optical density at 600 nm reached 1–1.5, and lipids were extracted with chloroform/methanol (C/M) as described (13, 14). The lipids were then dissolved in 1 ml of C/M (2:1, v/v), and 30 ml of ice-cold acetone was added. After a 20-min incubation on ice, the suspension was subjected to centrifugation at 1500 × *g* for 15 min at 1 °C, and the supernatant was carefully removed. The pellet was washed with ice-cold acetone, and the residue was dissolved in C/M (2:1, v/v). This was followed by fractionation by TLC using an Analtech TLC plate (Newark, DE) with a solvent system of C/M/acetone/acetic acid (90:10:10:1, v/v/v/v). The GMM fraction was extracted with C/M (2:1, v/v) from the silica gels. The preparative TLC and extraction procedure were repeated until no extra spots were detected on TLC plates. Finally, the GMM fraction was extracted with C/M (2:1, v/v), dried, and rinsed several times with methanol at room temperature to remove any residual contamination by glycopeptidolipids and phospholipids. The identity of the GMM preparation was confirmed by mass spectrometry. Protein contamination was not detected by silver staining of SDS-PAGE gels or by the Bradford assay. TDM was purified as described previously (14), and the *M. tuberculosis*-derived lipoarabinomannan was purchased from Nacalai Tesque.

Preparation of Liposomes—Stearylated octaarginine-containing liposomes were generated as described (15, 16) with slight modifications adapted for the integration of GMM. Briefly, purified GMMs in chloroform were mixed with egg phosphatidylcholine (NOF Corp., Tokyo, Japan), cholesterol (Avanti Polar Lipids, Alabaster, AL), and stearylated octaarginine (KURABO, Osaka, Japan) at a molar ratio of 7:3:0.5 in a test tube, and a lipid film was prepared by evaporating the solvent. Hydration of the lipid film was done by adding distilled water, and the total lipid concentration and the concentration were adjusted to 4 mM and 0.5 mg/ml, respectively. After the hydration, the mixture was sonicated gently for liposome formation. The efficiency of GMM integration into the liposomes ranged from 60 to 85%, as determined by TLC-based resolution of the lipids with a solvent system of C/M/acetone/acetic acid (90:10:10:1, v/v/v/v). The diameter of the liposomes was measured by dynamic light scattering, and the ζ-potential was determined by laser-Doppler velocimetry with a Zetasizer Nano (ZEN3600, Malvern Instruments, Ltd., Malvern, WR, UK). The diameter and ζ-potential of the GMM liposome were 120 ± 26 nm and 40 ± 8 mV, respectively, whereas those of empty liposome were 104 ± 10 nm and 38 ± 19 mV, respectively. TDM was incorporated into liposomes as for GMM, and its integration efficiency was 73.3%.

GMM-specific T Cell Assays—GMM-specific T cell assays using T cell receptor (TCR)-deficient Jurkat cells (J.RT3) reconstituted by transfection with GMM-specific, CD1-restricted TCRs (J.RT3/LDN5) have been described (17, 18). Human monocyte-derived dendritic cells and the C1R human B-lymphoblastoid cell line stably transfected with CD1b (C1R/CD1b), used as Ag-presenting cells in these assays, have also been described previously (17–19). The GMM liposome and the control (empty) liposome were dispersed in culture media just before use, whereas the purified GMM preparation was dispersed in the culture medium by sonication as in previous studies (17, 18, 20–23). The TCR-reconstituted J.RT3 cells (5×10^4/well) were cultured with irradiated Ag-presenting cells (5×10^4/well) in wells of 96-well, flat-bottomed microtiter plates in the presence of phorbol myristate acetate (10 ng/ml) and the indicated concentrations of Ag preparations. After 20 h, aliquots of the culture supernatants were collected, and the amount of IL-2 released into the supernatants was measured with the IL-2 ELISA kit (BD Biosciences).

Animals and Skin Tests—Three-week-old female Hartley guinea pigs were purchased from Japan SLC, Inc. (Shizuoka, Japan) and housed under specific pathogen-free conditions. The vaccine strain BCG Tokyo 172 (Japan BCG Laboratory) grown in 7H9 medium was harvested at its mid-log phase growth, and the viability was >70%. The bacteria were injected intradermally (5×10^7 colony-forming units per animal), and 6 weeks after infection, the skin on the left flank of guinea pigs was gently shaved and depilated for skin tests. Liposome containing 5 μg of GMM as well as an equivalent amount of empty liposome was dissolved in 100 μl of PBS and injected intradermally. A skin test with PPD (0.5 μg/site, Japan BCG Laboratory) was also performed in parallel. After the injection, the skin response was assessed at the indicated time points by measuring the distance across the skin induration. Experiments were repeated twice to confirm the reproducibility of the results. All animal experiments were performed according to institutional guidelines on animal welfare and the humane treatment of laboratory animals.

Histochemistry—The excised skin samples were fixed for 1 day with 4% paraformaldehyde, dehydrated, and embedded in paraffin. The tissue sections were stained with the hematoxylin and eosin solution (Merck) and observed under a microscope. Separately, some skin samples were deep-frozen in OCT compound (Sakura Finetechnical Co., Tokyo, Japan), and the cryosections were labeled with either mouse monoclonal antibodies

(mAbs) to guinea pig CD8 molecules (clone CT6; AbD Serotec, Oxford, UK) or those specifically recognizing guinea pig helper/inducer T cells (clone CT7; AbD Serotec) followed by incubation with FITC-conjugated donkey anti-mouse IgG Abs (Jackson ImmunoResearch Laboratories, Inc., West Grove, PA). After being washed, the labeled sections were mounted with Vectashield mounting medium (Vector Laboratories, Burlingame, CA) and viewed under a fluorescence microscope. Positive cells were counted in three randomly selected high power fields.

Cytokine mRNA Expression in GMM-stimulated Lymph Node Cells—Inguinal lymph node cells were isolated from BCG-immunized guinea pigs. The cells (2×10^6/well) were placed in wells of 96-well tissue culture plates and stimulated with either GMM in liposomes (1 μg/ml), TDM in liposomes (1 μg/ml), empty liposomes, lipoarabinomannan (1 μg/ml), or PPD (0.5 μg/ml) in RPMI1640 medium (Invitrogen) supplemented with 10% heat-inactivated FCS (Hyclone, Logan, UT). In some experiments the culture was performed in the presence of either the CD1F2/6B5 mouse mAb to guinea pig pan-group 1 CD1 molecules (24) or an isotype-matched control mAb (P3) (25) at a concentration of 10 μg/ml. After 18 h at 37 °C, the cells were harvested, and total RNA was extracted using the RNeasy mini kit (Qiagen, Hilden, Germany). The first-strand cDNA was synthesized from 0.1–0.5 μg of total RNA using oligo(dT) and the PrimeScript reverse transcriptase (Takara Bio, Inc., Otsu, Japan). To amplify specific transcripts, the samples were subjected to PCR for 35 cycles of 1 min at 94 °C, 1 min at 60 °C (63 °C for IL-5), and 1 min at 72 °C followed by a 10-min incubation at 72 °C. The primers used were: 5′-CTA GCT ACT ACT GCC AGT CAA GAT-3′ (sense) and 5′-GCT CTG AAA CAG CAT CTG AGT CCT-3′ (antisense) for IFN-γ; 5′-CCA TGA GCA CAG AAA GCA TGA TCC G-3′ (sense) and 5′-CTC ACA GGG CAA TGA CCC CAA AGT A-3′ (antisense) for TNF-α; 5′-CCA TGA GGG TGC TTC TGC AGT TGG G-3′ (sense) and 5′-CTC AGC CTT CAA TTG TCC ATT CCG T-3′ (antisense) for IL-5; 5′-GGC ACG AAC ACC CAG TCT GA-3′ (sense) and 5′-TCA CCT GCT CCA CTG CCT TG-3′ (antisense) for IL-10. The PCR products were resolved on 1.2% agarose gels and visualized by staining with ethidium bromide and UV transillumination. The experiments were repeated at least twice to confirm the reproducibility of the results.

Statistical Analysis—The statistical analysis was performed using Student's *t* test. *p* values of < 0.05 were considered statistically significant.

RESULTS

Increased Efficiency of GMM Presentation after Incorporation into Liposomes—The GMM produced by pathogenic mycobacteria contains mycolic acids with extremely long carbon chains (C_{80-90}) and can be dissolved in chloroform. In T cell assays performed in previous studies, including ours (17, 18, 20–23), GMM was forced to disperse temporarily into aqueous media by sonication, but because of its highly hydrophobic properties, it is possible that the form of GMM prepared by this method may not be utilized efficiently for the presentation of Ags. Therefore, we incorporated GMM into liposomes constructed

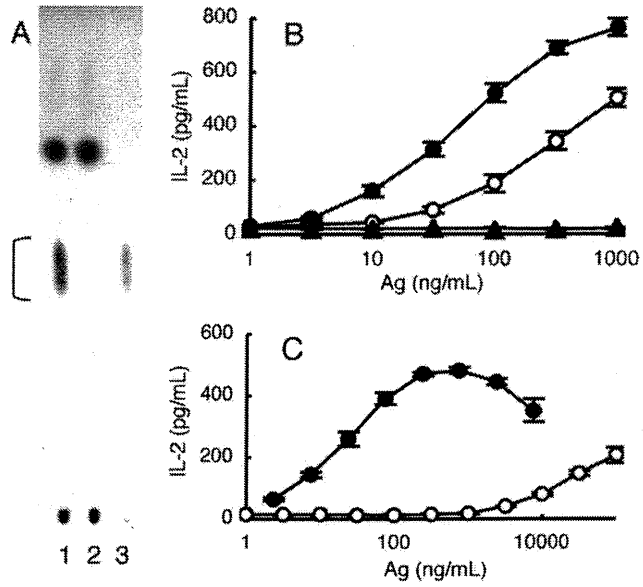

FIGURE 1. **Efficient presentation of GMM encapsulated in liposomes.** *A*, lipids present in the GMM liposome (*lane 1*) and the empty liposome (*lane 2*) were resolved on a TLC plate and visualized by spraying 50% sulfuric acid and baking. The reference GMM was also resolved in parallel (*lane 3*), and the position of GMM was indicated with a *bracket*. *B*, the GMM-specific TCR-reconstituted J.RT3/LDN5 cells were stimulated with the indicated concentrations of GMM either prepared by sonication (*open circles*) or encapsulated in liposomes (*closed circles*) using monocyte-derived dendritic cells as Ag-presenting cells. An empty liposome that contained the corresponding amounts of the framework lipids but lacked incorporated GMM was used as a control (*closed triangles*). The GMM-specific response was monitored by measuring the amount of IL-2 secreted into the culture medium. *C*, the J.RT3/LDN5 cells were stimulated with GMM either prepared by sonication (*open circles*) or encapsulated in liposomes (*closed circles*) using $CD1b^+$ human B-lymphoblastoid cells as Ag-presenting cells.

by defined phospholipids, cholesterol, and stearylated octaarginine. A TLC-based analysis revealed that the GMM liposome (Fig. 1*A*, *lane 1*), but not empty liposome (*lane 2*), contained a lipid (indicated with a *bracket*) that comigrated with the reference GMM (*lane 3*), confirming the integration of GMM. We then compared Ag presentation efficiency of the GMM liposome with that of the sonicated GMM preparation used frequently in previous studies (10, 18, 21, 22, 26). In the presence of monocyte-derived dendritic cells, the J.RT3/LDN5 cells expressing GMM-specific, CD1b-restricted TCRs secreted IL-2 in response to the sonicated GMM preparation in a dose-dependent manner (Fig. 1*B*, *open circles*). Strikingly, an ~10-fold more efficient T cell activation was observed when GMM was applied in the form of liposomes (*closed circles*), whereas no T cell activation was detected when the empty liposome was added (*closed triangles*). GMM incorporated in liposomes was also presented efficiently by a CD1b-transfected B-lymphoblastoid cell line (C1R/CD1b) (Fig. 1*C*, *closed circles*) that was of a cell type relatively inefficient in utilizing the sonicated GMM preparation (*open circles*). These results as well as its high solubility in aqueous solutions suggested that the GMM liposome might be useful for eliciting specific T cell responses *in vivo*.

Skin DTH Reactions Elicited by the GMM Liposome—In our previous study (9), in which TDM-elicited eosinophilic skin hypersensitivity was demonstrated in mycobacteria-infected guinea pigs, the intradermal administration of GMM in mineral

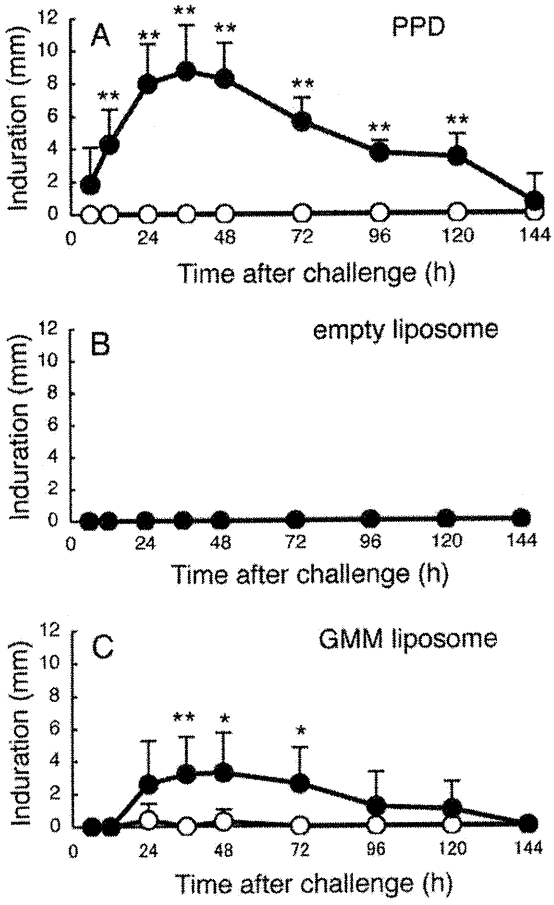

FIGURE 2. **Induction of GMM-elicited DTH reactions in BCG-vaccinated guinea pigs.** *A*, six BCG-vaccinated (*filled circles*) and six mock-vaccinated (*open circles*) guinea pigs received an intradermal injection of either 0.5 μg of PPD (*A*), 5 μg of the GMM liposome (*C*), or the corresponding amount of the empty liposome (*B*), and at the indicated time points after the challenge, the diameter of the skin induration was measured (*, $p < 0.05$; **, $p < 0.01$).

oil failed to induce any significant skin responses. Given the highly efficient T cell-activating capacity of the GMM liposome, we set up an experiment in which BCG-vaccinated and mock-vaccinated guinea pigs were tested for skin reactions to the liposome. Six weeks after the vaccination, either PPD, empty liposome, or the GMM liposome was injected intradermally, and the local induration at the site of challenge was monitored. Consistent with the classical DTH response, a skin reaction to PPD was observed in BCG-vaccinated (Fig. 2*A*, *closed circles*), but not mock-vaccinated (*open circles*), animals with a peak at 36–48 h. Whereas no response was elicited toward the empty liposome (Fig. 2*B*), significant induration was observed at the site of challenge with the GMM liposome in BCG-vaccinated (Fig. 2*C*, *closed circles*), but not mock-vaccinated (*open circles*), guinea pigs with the peak response reached around 48 h. Thus, the skin reaction to the GMM liposome was comparable with the PPD skin reaction in terms of both requirement for sensitization with BCG and the "delayed-type" response.

Histological analysis further pointed to substantial similarities between the PPD-elicited and GMM-elicited skin reactions. As expected, the response to PPD in BCG-vaccinated animals involved infiltration by mononuclear cells (Fig. 3*B*). The skin response to the GMM liposome (Fig. 3*J*) in these animals was also associated with a mononuclear cell mobilization that was apparently indistinguishable from the PPD-evoked response. It should also be noted that no significant histological changes were induced in the empty liposome-challenged skin of BCG-vaccinated guinea pigs (Fig. 3*F*) or in the GMM liposome-challenged skin of mock-vaccinated guinea pigs (Fig. 3*I*), suggesting that the GMM liposome-elicited response in BCG-vaccinated animals requires both BCG sensitization and the GMM challenge to occur.

Guinea pig T cells were roughly subdivided into $CT7^+$ helper/inducer T cells and $CT6^+$ killer T cells, based on their reactivity to commercial mAb clones, CT7 and CT6, respectively (9, 27). We carried out immunohistological analyses with these mAbs (Fig. 3, *panels on the right*) and determined the number of these cells in the challenged skin (Fig. 4). The absolute number of $CT7^+$ cells was significantly increased in the GMM-challenged skin of BCG-vaccinated animals as compared with that in the GMM-challenged skin of mock-vaccinated animals and in mock-challenged skin of BCG-vaccinated animals (Fig. 4*A*). The absolute number of $CT6^+$ cells was also increased significantly in the GMM-challenged skin of BCG-vaccinated animals as compared with the relevant controls (Fig. 4*B*). An increase in the number of $CT7^+$ and $CT6^+$ cells was also observed in the PPD-challenged skin of BCG-vaccinated animals (Fig. 4, *A* and *B*), and therefore, no apparent differences were observed in the infiltrating T cell subsets for the PPD-elicited and GMM-elicited skin hypersensitivity.

The Group 1 CD1-dependent Response to GMM in BCG-vaccinated Guinea Pigs—GMM-specific T cell activation depends on the function of CD1b or related group 1 CD1 molecules in humans (5), monkeys (28), and cows (29). Therefore, it would be reasonable to speculate that the GMM-elicited response in BCG-vaccinated guinea pigs was restricted to guinea pig group 1 CD1 molecules. To address this, mononuclear cells were obtained from the draining lymph nodes of BCG-vaccinated guinea pigs and stimulated *in vitro* with the GMM liposome in the presence or absence of the CD1F2/6B5 anti-pan guinea pig group 1 CD1 mAb. This was followed by detection of IFN-γ transcription by RT-PCR. Prominent transcription of IFN-γ was detected when the cells were stimulated with the GMM liposome, but not with the empty liposome, and the GMM liposome-elicited IFN-γ response was totally abrogated when the cells were cultured in the presence of the CD1F2/6B5 blocking mAb but not the isotype-matched control mAb (Fig. 5*A*). Thus, these results confirmed that the GMM-specific response induced in the BCG-vaccinated guinea pigs was dependent on the function of group 1 CD1 molecules.

Highly Biased Th1-type Cytokine Expression Elicited by GMM—It has been established that Th1-type cytokines, such as IFN-γ and TNF-α, are critical for host defense against tuberculosis, and Th2-type cytokines may potentially counteract the Th1-type responses to aggravate the disease (30). To gain insights into the significance of the GMM-elicited hypersensitivity, mononuclear cells isolated from the draining lymph nodes of BCG-vaccinated guinea pigs were stimulated with specific Ags, and cytokine profiles were determined by RT-PCR.

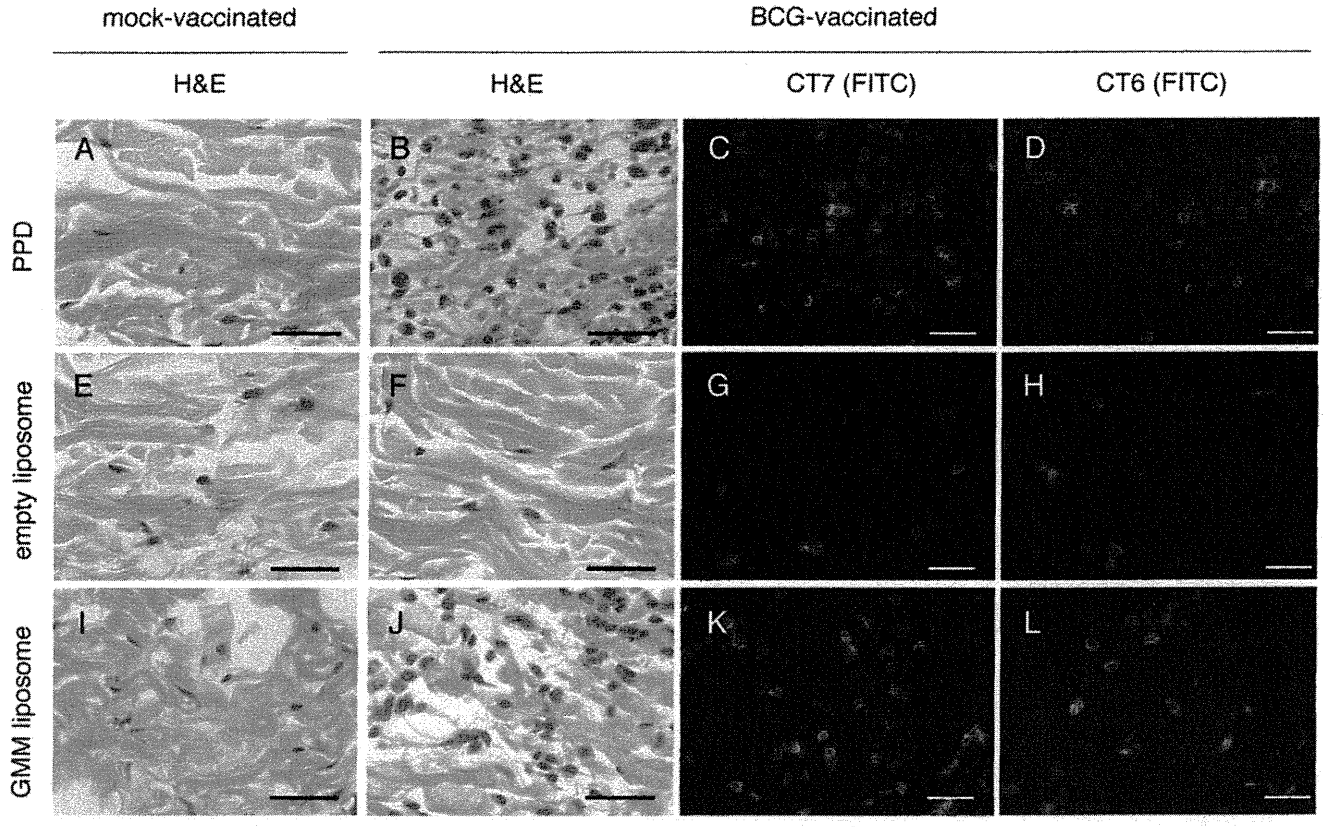

FIGURE 3. **Infiltration by mononuclear cells at the site of the GMM-elicited DTH.** BCG-vaccinated and mock-vaccinated guinea pigs received an intradermal injection of either PPD (*A–D*), the empty liposome (*E–H*), or the GMM liposome (*I–L*), and after 48 h, the challenged skin specimens were subjected to hematoxylin and eosin (*H&E*) staining (*panels on the left*) as well as immunostaining (*panels on the right*) with indicated mAbs. *Scale bars*, 50 μm.

PPD-stimulated cells showed increased levels of not only Th1-type cytokines, IFN-γ, and TNF-α but also Th2-type cytokines, IL-5 and IL-10 (Fig. 5*B*, *right panels*). In sharp contrast, only the Th1-type cytokines were detected in cells stimulated with GMM (Fig. 5*B*, *left panels*). These results suggest that, as compared with the classical DTH directed against PPD or the tuberculin skin test, the GMM-elicited DTH is more biased toward Th1-type responses. Furthermore, the lymph node cells stimulated with other mycobacteria-derived glycolipids, TDM and lipoarabinomannan, up-regulated the expression of IL-10 (Fig. 5*C*), highlighting the unique capacity for GMM to elicit highly Th1-skewed responses.

DISCUSSION

We have previously detected mycobacteria-specific, group 1 CD1-restricted "memory-type" T cell responses in BCG-vaccinated human individuals and guinea pigs (26, 27). The existence of lipid-specific memory-type T cells is also supported by the finding that vaccination with mycobacteria-derived lipids confers resistance to tuberculosis in guinea pigs (8). Nevertheless, the hypersensitivity to mycobacteria-derived lipid components that is comparable with the DTH to PPD, a hallmark of mycobacterial infection in immunocompetent individuals, has been poorly understood. Initially, we observed the TDM-elicited eosinophilic hypersensitivity that was distinct from the classical DTH response to protein Ags and failed to detect apparent hypersensitivity reactions to GMM dissolved in mineral oil (9). With the alternative use of the GMM liposome (Fig. 1), however, the present study now detects a DTH response to GMM that is comparable both in time course (Fig. 2) and in infiltrating cell types (Figs. 3 and 4) to the classical DTH reactions to protein Ags. Therefore, the present study identifies CD1-presented microbial glycolipids as a new chemical class of target Ags to which DTH is directed. Furthermore, given the apparently skewed Th1-type cytokine response as compared with the response to PPD (Fig. 5), the DTH reaction representing high levels of GMM-specific T cell responses could potentially function as an alternative and even more accurate indicator for cell-mediated immunity against tuberculosis. Mycobacteria-derived lipid Ags presented by CD1 molecules are highly hydrophobic, and therefore, the T cell response to these Ags has been difficult to prove *in vivo* due to their insolubility in aqueous solutions. The present study successfully utilized octaarginine-modified liposomes that had high affinity to cellular membranes and were efficiently internalized by a variety of cells (16, 31). Moreover, the GMM liposome was designed for efficient delivery to lysosomes, where Ag loading onto CD1b molecules was proposed to occur (32), by using non-fusogenic lipids, such as egg phosphatidylcholine and cholesterol. Thus, the liposome design used in this study will be useful for the development of lipid-based vaccines and skin tests as proposed below.

Pathogenic mycobacteria grown in standard culture media produce a large quantity of TDM with only a scarce amount of

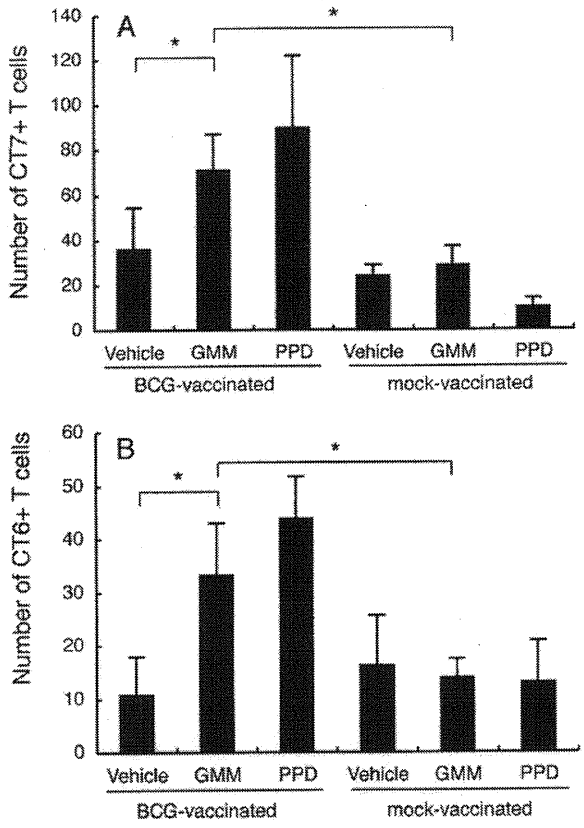

FIGURE 4. **Increased numbers of CT7$^+$ and CT6$^+$ T cells at the site of the GMM-elicited DTH.** Frozen sections of the empty liposome-challenged skin, the GMM liposome-challenged skin, and the PPD-challenged skin in BCG-vaccinated as well as mock-vaccinated guinea pigs were stained with either the mAb CT7 for detection of helper/inducer cells or the mAb CT6 for detection of killer T cells. The numbers of CT7$^+$ cells (*A*) and CT6$^+$ cells (*B*) were determined by counting positively labeled cells in three randomly selected high power fields (*, $p < 0.01$).

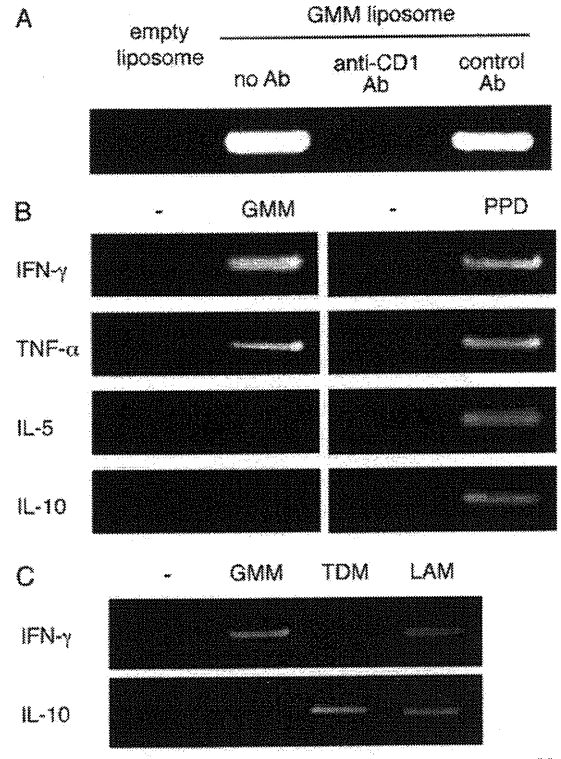

FIGURE 5. ***In vitro* response of BCG-vaccinated guinea pig-derived lymph node cells to the GMM liposome.** *A*, draining lymph node cells were isolated from BCG-vaccinated guinea pigs and stimulated *in vitro* with either the empty liposome or the GMM liposome. GMM stimulation was also performed in the presence of either the CD1F2/6B5 anti-pan guinea pig CD1 mAb or an isotype-matched control mAb (clone P3). After 18 h, the cells were harvested, total RNA was extracted, and RT-PCR was performed to detect IFN-γ transcription. *B*, the lymph node cells were stimulated *in vitro* with either the GMM liposome or PPD, and RT-PCR was performed as in *A* to detect the transcription of Th1-type cytokines (IFN-γ and TNF-α) and Th2-type cytokines (IL-5 and IL-10). *C*, the lymph node cells were stimulated with either the GMM liposome, the TDM liposome, or lipoarabinomannan, and RT-PCR was performed to detect the IFN-γ and IL-10 transcription.

GMM, and therefore, TDM has been proposed as a major surface-exposed mycolylglycolipid in a prototypic model of the cell wall of mycobacteria (33). Immunologists, however, predict that this model may not represent pathogenic mycobacteria interacting with the host because TDM-rich mycobacteria would be easily detected and eliminated by innate immune cells expressing specific receptors, such as Mincle (34). Our recent study (10, 35) determining the pathway of GMM biosynthesis provided a clue to this enigma. Mycolyltransferases, or Ag85, mediate the final step of TDM biosynthesis by transferring a mycolate group from trehalose monomycolate captured at the donor site to trehalose monomycolate at the acceptor site. In glucose-rich environments, such as those in the host, glucose competitively gains access to the acceptor site of the enzymes and acquires a mycolate group transferred from the donor trehalose monomycolate, resulting in the biosynthesis of GMM and down-regulation of TDM production. Given that GMM is much less potent than TDM in stimulating innate immune cells (10), the switch from TDM to GMM biosynthesis by utilizing pre-existing enzymes and borrowing host-derived glucose could quickly allow the microbes to avoid the host innate immune system. GMM-expressing mycobacteria that have broken the frontline of defense mediated by innate immunity are then faced with adaptive immunity directed against GMM. A human GMM-specific T cell line, LDN5, is capable of recognizing mycobacteria-infected dendritic cells and eliminating the infected cells in a Fas-dependent fashion (7). Furthermore, as demonstrated in the present study, high levels of specific T cell responses are evoked after sensitization, which are associated with the production of IFN-γ and TNF-α, the two major cytokines that control mycobacterial infections. These findings as well as the observation that the GMM-specific T cell response preferentially occurs in live infections raise the possibility that the DTH response to GMM participates in host immunity against tuberculosis.

Obviously, an important extension of this line of study would be the development of lipid-based subunit vaccines, such as GMM, against human tuberculosis. CD1 genes lack the polymorphisms seen for MHC genes (36), and therefore, the emergence of specific haplotype-associated low responder populations would be minimized with lipid vaccines. Related to vaccine development, the issue of whether the "GMM skin test" could substitute for the tuberculin test should also be addressed from a variety of medical and pharmaceutical standpoints. Par-

ticularly, it has been proposed that a positive tuberculin test does not necessarily correlate with resistance against tuberculosis, limiting the value of the tuberculin test for diagnosis, and therefore, a critical issue to address is whether a positive GMM skin test can function as an accurate and convenient indicator for established host immunity against human tuberculosis. The present study unravels previously undefined tuberculosis-associated DTH responses that may have important medical implications.

Acknowledgment—We thank Dr. Ikuya Yano (Japan BCG laboratory) for providing valuable materials.

REFERENCES

1. Kobayashi, K., Kaneda, K., and Kasama, T. (2001) *Microsc. Res. Tech.* **53,** 241–245
2. Orme, I. M., and Cooper, A. M. (1999) *Immunol. Today* **20,** 307–312
3. Behar, S. M., and Porcelli, S. A. (2007) *Curr. Top. Microbiol. Immunol.* **314,** 215–250
4. Moody, D. B., Ulrichs, T., Mühlecker, W., Young, D. C., Gurcha, S. S., Grant, E., Rosat, J. P., Brenner, M. B., Costello, C. E., Besra, G. S., and Porcelli, S. A. (2000) *Nature* **404,** 884–888
5. Ulrichs, T., Moody, D. B., Grant, E., Kaufmann, S. H., and Porcelli, S. A. (2003) *Infect. Immun.* **71,** 3076–3087
6. Stenger, S., Hanson, D. A., Teitelbaum, R., Dewan, P., Niazi, K. R., Froelich, C. J., Ganz, T., Thoma-Uszynski, S., Melián, A., Bogdan, C., Porcelli, S. A., Bloom, B. R., Krensky, A. M., and Modlin, R. L. (1998) *Science* **282,** 121–125
7. Stenger, S., Mazzaccaro, R. J., Uyemura, K., Cho, S., Barnes, P. F., Rosat, J. P., Sette, A., Brenner, M. B., Porcelli, S. A., Bloom, B. R., and Modlin, R. L. (1997) *Science* **276,** 1684–1687
8. Dascher, C. C., Hiromatsu, K., Xiong, X., Morehouse, C., Watts, G., Liu, G., McMurray, D. N., LeClair, K. P., Porcelli, S. A., and Brenner, M. B. (2003) *Int. Immunol.* **15,** 915–925
9. Otsuka, A., Matsunaga, I., Komori, T., Tomita, K., Toda, Y., Manabe, T., Miyachi, Y., and Sugita, M. (2008) *J. Immunol.* **181,** 8528–8533
10. Matsunaga, I., Naka, T., Talekar, R. S., McConnell, M. J., Katoh, K., Nakao, H., Otsuka, A., Behar, S. M., Yano, I., Moody, D. B., and Sugita, M. (2008) *J. Biol. Chem.* **283,** 28835–28841
11. Batuwangala, T., Shepherd, D., Gadola, S. D., Gibson, K. J., Zaccai, N. R., Fersht, A. R., Besra, G. S., Cerundolo, V., and Jones, E. Y. (2004) *J. Immunol.* **172,** 2382–2388
12. Moody, D. B., Reinhold, B. B., Guy, M. R., Beckman, E. M., Frederique, D. E., Furlong, S. T., Ye, S., Reinhold, V. N., Sieling, P. A., Modlin, R. L., Besra, G. S., and Porcelli, S. A. (1997) *Science* **278,** 283–286
13. Hiromatsu, K., Dascher, C. C., LeClair, K. P., Sugita, M., Furlong, S. T., Brenner, M. B., and Porcelli, S. A. (2002) *J. Immunol.* **169,** 330–339
14. Matsunaga, I., Bhatt, A., Young, D. C., Cheng, T. Y., Eyles, S. J., Besra, G. S., Briken, V., Porcelli, S. A., Costello, C. E., Jacobs, W. R., Jr., and Moody, D. B. (2004) *J. Exp. Med.* **200,** 1559–1569
15. Homhuan, A., Kogure, K., Nakamura, T., Shastri, N., and Harashima, H. (2009) *J. Control Release* **136,** 79–85
16. Nakamura, T., Moriguchi, R., Kogure, K., Shastri, N., and Harashima, H. (2008) *Mol. Ther.* **16,** 1507–1514
17. Grant, E. P., Degano, M., Rosat, J. P., Stenger, S., Modlin, R. L., Wilson, I. A., Porcelli, S. A., and Brenner, M. B. (1999) *J. Exp. Med.* **189,** 195–205
18. Sugita, M., Grant, E. P., van Donselaar, E., Hsu, V. W., Rogers, R. A., Peters, P. J., and Brenner, M. B. (1999) *Immunity* **11,** 743–752
19. Sugita, M., Porcelli, S. A., and Brenner, M. B. (1997) *J. Immunol.* **159,** 2358–2365
20. Rosat, J. P., Grant, E. P., Beckman, E. M., Dascher, C. C., Sieling, P. A., Frederique, D., Modlin, R. L., Porcelli, S. A., Furlong, S. T., and Brenner, M. B. (1999) *J. Immunol.* **162,** 366–371
21. Sugita, M., Cao, X., Watts, G. F., Rogers, R. A., Bonifacino, J. S., and Brenner, M. B. (2002) *Immunity* **16,** 697–706
22. Sugita, M., van Der Wel, N., Rogers, R. A., Peters, P. J., and Brenner, M. B. (2000) *Proc. Natl. Acad. Sci. U.S.A.* **97,** 8445–8450
23. Moody, D. B., Guy, M. R., Grant, E., Cheng, T. Y., Brenner, M. B., Besra, G. S., and Porcelli, S. A. (2000) *J. Exp. Med.* **192,** 965–976
24. Hiromatsu, K., Dascher, C. C., Sugita, M., Gingrich-Baker, C., Behar, S. M., LeClair, K. P., Brenner, M. B., and Porcelli, S. A. (2002) *Immunology* **106,** 159–172
25. Hochstenbach, F., David, V., Watkins, S., and Brenner, M. B. (1992) *Proc. Natl. Acad. Sci. U.S.A.* **89,** 4734–4738
26. Kawashima, T., Norose, Y., Watanabe, Y., Enomoto, Y., Narazaki, H., Watari, E., Tanaka, S., Takahashi, H., Yano, I., Brenner, M. B., and Sugita, M. (2003) *J. Immunol.* **170,** 5345–5348
27. Watanabe, Y., Watari, E., Matsunaga, I., Hiromatsu, K., Dascher, C. C., Kawashima, T., Norose, Y., Shimizu, K., Takahashi, H., Yano, I., and Sugita, M. (2006) *Vaccine* **24,** 5700–5707
28. Morita, D., Katoh, K., Harada, T., Nakagawa, Y., Matsunaga, I., Miura, T., Adachi, A., Igarashi, T., and Sugita, M. (2008) *Biochem. Biophys. Res. Commun.* **377,** 889–893
29. Van Rhijn, I., Nguyen, T. K., Michel, A., Cooper, D., Govaerts, M., Cheng, T. Y., van Eden, W., Moody, D. B., Coetzer, J. A., Rutten, V., and Koets, A. P. (2009) *Eur. J. Immunol.* **39,** 3031–3041
30. North, R. J., and Jung, Y. J. (2004) *Annu. Rev. Immunol.* **22,** 599–623
31. Khalil, I. A., Kogure, K., Futaki, S., and Harashima, H. (2006) *J. Biol. Chem.* **281,** 3544–3551
32. Sugita, M., Jackman, R. M., van Donselaar, E., Behar, S. M., Rogers, R. A., Peters, P. J., Brenner, M. B., and Porcelli, S. A. (1996) *Science* **273,** 349–352
33. Ryll, R., Kumazawa, Y., and Yano, I. (2001) *Microbiol. Immunol.* **45,** 801–811
34. Ishikawa, E., Ishikawa, T., Morita, Y. S., Toyonaga, K., Yamada, H., Takeuchi, O., Kinoshita, T., Akira, S., Yoshikai, Y., and Yamasaki, S. (2009) *J. Exp. Med.* **206,** 2879–2888
35. Nakao, H., Matsunaga, I., Morita, D., Aboshi, T., Harada, T., Nakagawa, Y., Mori, N., and Sugita, M. (2009) *J. Biochem.* **146,** 659–665
36. Porcelli, S. A. (1995) *Adv. Immunol.* **59,** 1–98

Journal of Medical Microbiology (2011), 60, 582–591 DOI 10.1099/jmm.0.026047-0

Expression of the *Mycobacterium tuberculosis* PPE37 protein in *Mycobacterium smegmatis* induces low tumour necrosis factor alpha and interleukin 6 production in murine macrophages

Sylvia Daim, Ikuo Kawamura, Kohsuke Tsuchiya, Hideki Hara, Takeshi Kurenuma, Yanna Shen, Sita R. Dewamitta, Shunsuke Sakai, Takamasa Nomura, Huixin Qu and Masao Mitsuyama

Department of Microbiology, Kyoto University Graduate School of Medicine, Yoshida Konoe-cho, Sakyo-ku, Kyoto 606-8501, Japan

Correspondence
Ikuo Kawamura
ikuo_kawamura@mb.med.kyoto-u.ac.jp

Received 9 September 2010
Accepted 10 January 2011

PPE37 is a member of the *Mycobacterium tuberculosis* proline-proline-glutamic acid (PPE) multigene family. Its expression is upregulated in bacteria that are phagocytosed by macrophages and is enhanced even more in bacteria isolated from the lungs of infected mice. This raises the possibility that PPE37 may play a role in the virulence of *M. tuberculosis* and led to this investigation of the function of PPE37. Recombinant bacterial strains, one expressing the *M. tuberculosis* PPE37 protein (Ms_ppe37) and another harbouring the vector alone (Ms_vec) were generated from the non-pathogenic *Mycobacterium smegmatis*. These bacterial strains were used to infect peritoneal exudate and bone marrow-derived macrophages. It was found that, despite the comparable intracellular survival between the two recombinant *M. smegmatis* strains, Ms_ppe37 induced a significantly lower level of tumour necrosis factor alpha and interleukin 6 in the infected macrophages compared with Ms_vec. Western blot analyses revealed that the activation levels of nuclear factor kappa B, mitogen-activated protein kinase (MAPK)/extracellular signal-regulated kinase and MAPK/p38 were lower in macrophages infected with Ms_ppe37 than in macrophages infected with Ms_vec. These results suggest that PPE37 may have a potential role in interfering with the pro-inflammatory cytokine response of infected macrophages.

INTRODUCTION

The existence of the proline-proline-glutamic acid (PPE) multigene family was revealed when the decoding of the *Mycobacterium tuberculosis* genome was completed (Cole *et al.*, 1998). Members of this gene family were found to share a highly conserved N-terminal sequence of approximately 180 aa that also contained the conserved PPE motif. In contrast, their C-terminal regions were highly heterogeneous in both sequence and length (Cole *et al.*, 1998). The *ppe* genes are not found outside the genus *Mycobacterium* and are highly distributed among the pathogenic species of mycobacteria (Gey van Pittius *et al.*, 2006). For these reasons, they are speculated to contribute to the pathogenicity of *M. tuberculosis*. A possible functional role has been proposed for the PPE proteins, in which they serve as a source of antigenic variation that promotes antigenic diversity in *M. tuberculosis* (Cole *et al.*, 1998). Indeed, the PPE proteins reported to date are immunogenic, eliciting either humoral or T-cell immune responses (Choudhary *et al.*, 2003; Khan *et al.*, 2008; Romano *et al.*, 2008; Tundup *et al.*, 2008; Wang *et al.*, 2008).

One of the PPE proteins, PPE37, may have a role in the virulence of *M. tuberculosis*. It has been reported that expression of the *ppe37* gene is upregulated in *M. tuberculosis* during infection of murine bone marrow-derived macrophages (Schnappinger *et al.*, 2003; Voskuil *et al.*, 2004). Moreover, in *M. tuberculosis* isolated from the lungs of infected mice, expression of the *ppe37* gene is enhanced even more (Schnappinger *et al.*, 2003). Earlier studies have shown that an iron-dependent transcriptional regulator that is critical for proper iron homeostasis in *M. tuberculosis* regulates the expression of *ppe37* (Rodriguez *et al.*, 1999, 2002). When *M. tuberculosis* was exposed to iron-limiting conditions in *in vitro* culture, the expression of *ppe37* increased greatly (Rodriguez *et al.*, 2002; Schnappinger *et al.*, 2003). In addition, *in vitro* exposure of *M. tuberculosis* to nitrosative and oxidative growth conditions also increased the expression of *ppe37* (Schnappinger *et al.*, 2003; Voskuil *et al.*, 2004). Both of

Abbreviations: ERK, extracellular signal-regulated kinase; IL, interleukin; LDH, lactate dehydrogenase; MAPK, mitogen-activated protein kinase; MHC, major histocompatibility complex; NF-κB, nuclear factor kappa B; TNF-α, tumour necrosis factor alpha; TLR, Toll-like receptor.

these conditions are reported to mimic the macrophage phagosomal environment that contains *M. tuberculosis* (Schnappinger *et al.*, 2003). From these results, it seems that PPE37 is required for the adaptation of *M. tuberculosis* to the intracellular niche in macrophages.

In the present study, as a first step towards evaluating the possible role of PPE37 in the virulence of *M. tuberculosis*, we took advantage of the lack of *ppe* genes in *Mycobacterium smegmatis* and generated two recombinant bacterial strains using this non-pathogenic bacterium. Unlike the *M. tuberculosis* genome, which contains 69 *ppe* ORFs, the *M. smegmatis* genome contains only 2. Furthermore, none of the *M. smegmatis ppe* genes are orthologues of the *M. tuberculosis ppe37* gene (Gey van Pittius *et al.*, 2006). We cloned the *ppe37* gene from the *M. tuberculosis* strain H37Rv and expressed the gene in *M. smegmatis* strain mc^2 155 (Ms_ppe37). The ability of Ms_ppe37 to survive inside macrophages was assessed in *in vitro* infection of mouse macrophages. In addition, the effect of PPE37 on the macrophage cytokine response was also investigated.

METHODS

Bacterial strains and growth conditions. *Escherichia coli* DH5α was routinely grown in Lennox LB medium for use in DNA cloning procedures. *M. tuberculosis* strain H37Rv and *M. smegmatis* strain mc^2 155 were grown at 37 °C in Middlebrook 7H9 liquid medium or on Middlebrook 7H10 agar (Difco) supplemented with 0.5 % (w/v) albumin fraction V, 0.2 % (w/v) glucose, 0.5 % (v/v) glycerol and 0.05 % (v/v) Tween 80. For the preparation of culture filtrate fraction, recombinant *M. smegmatis* Ms_ppe37 was grown in Sauton medium as described by Rosenkrands & Andersen (2001). When required, 25 μg kanamycin ml^{-1} was also added.

Macrophages. C57BL/6 female mice of 7 to 9 weeks old (Japan SLC) were used in experiments according to protocols approved by the Animal Ethics and Research Committee of Kyoto University Graduate School of Medicine. Peritoneal exudate cells were harvested from mice 3–4 days after intraperitoneal injection with 2.5 ml 3 % (w/v) thioglycollate (Eiken Chemical). Cells were washed, seeded in tissue culture plates and cultured for 2 h in 5 % CO_2 at 37 °C in RPMI 1640 supplemented with 10 % (v/v) heat-inactivated fetal bovine serum. Adherent cells were used as peritoneal exudate macrophages after non-adherent cells had been removed by washing. In other experiments, bone marrow cells were collected from the tibiae of mice. Cells were cultured for 5–7 days in RPMI 1640 supplemented with 10 % heat-inactivated fetal bovine serum, 20 μg gentamicin ml^{-1} and 100 ng mouse macrophage colony-stimulating factor ml^{-1} (R&D Systems). After removal of non-adherent cells, adherent cells were used as bone marrow-derived macrophages.

Generation of recombinant *M. smegmatis* expressing PPE37. Chromosomal DNA was isolated from *M. tuberculosis*, and the *ppe37* gene was PCR-amplified with the use of forward primer 5′-TTACTAGTcaccatcacACCTTCCCGAT-3′ containing an *SpeI* site (underlined) and three His codons (lower-case letters), and reverse primer 5′-CCGTAAGCTTCTTCAACGTTTAATCTGACC-3′ containing a *Hin*dIII site (underlined). The PCR product of approximately 1.5 kb was cloned into the pEGFP vector (Clontech Laboratories), generating the recombinant plasmid pEGFP-his3ppe37. Three additional His codons were introduced at the 5′ end of the his3ppe37 sequence with the use of the same reverse primer and a second forward primer, 5′-TGAATTCATGcatcaccatcaccatcacACC-3′, containing an *Eco*RI site (underlined) and the His codons (lower-case letters). The resultant PCR product containing six consecutive His codons was inserted in frame into the cloning site of pMV261, a mycobacterial expression vector (Stover *et al.*, 1991), generating pMV261-his6ppe37. The recombinant plasmid or empty pMV261 was electroporated into *M. smegmatis* mc^2 155 according to standard procedures (Larsen, 2000). Recombinant *M. smegmatis* expressing 6His-tagged PPE37 (Ms_ppe37) and *M. smegmatis* harbouring empty pMV261 alone (Ms_vec) were selected on Middlebrook 7H10 agar containing 25 μg kanamycin ml^{-1}.

Detection of *ppe37* gene expression in recombinant *M. smegmatis*. Recombinant *M. smegmatis* strains were cultured until they reached an OD_{600} of 0.6–1.0 in 100 ml Middlebrook 7H9 liquid medium in the presence of 25 μg kanamycin ml^{-1}. Total bacterial RNA was isolated using Sepasol RNA I Super (Nacalai Tesque). All RNA samples were treated with DNase I (Promega) and subjected to PCR to test for the complete removal of genomic DNA. cDNA was synthesized from 1 μg total RNA in a 40 μl reaction mix containing reverse transcriptase buffer, 150 ng random primers, 2 μl 10 mM dNTP mix, 2 μl 0.1 M DTT and 400 U SuperScript III reverse transcriptase (Invitrogen). PCR was performed with a KOD-Plus enzyme kit (Toyobo) and the following primer pairs: (i) *ppe37* gene – 5′-TGTTGGACTGGTTCATCTCG-3′ (forward) and 5′-CAGTCT-TGTTGCTTTGCTGG-3′ (reverse), product size 500 bp; and (ii) aminoglycoside phosphotransferase (*aph*) gene – 5′-AGGTAGC-GTTGCCAATGATG-3′ (forward) and 5′-CTCACCGAGGCAGTT-CCATA-3′ (reverse), product size 540 bp.

Detection of His-tagged PPE37. Recombinant *M. smegmatis* strains were cultured to an OD_{600} of 0.6–1.0 in 25 ml Middlebrook 7H9 liquid medium or 50 ml Sauton medium in the presence of 25 μg kanamycin ml^{-1}. Bacterial pellets were harvested, washed three times with ice-cold PBS and resuspended in extraction buffer containing 20 mM Tris/HCl (pH 6.8), 4 mM EDTA, 0.6 % SDS and protease inhibitor cocktail (Nacalai Tesque). Bacterial cells were disrupted and supernatants were collected after centrifugation at 20 000 ***g*** for 20 min at 4 °C. For preparation of the culture filtrate fraction, the culture supernatant of bacteria grown in Sauton medium was harvested by centrifugation at 2000 ***g*** for 15 min at 4 °C. The supernatant was filtered through a 0.2 μm syringe filter and concentrated to approximately 150 μl using a centrifugal filter with a cut-off value of 5 kDa (Millipore). Samples were subjected to SDS-PAGE, and the His-tagged PPE37 protein was detected by Western blotting and mouse anti-penta-His antibody (Qiagen). Chemiluminescent images were captured with a luminescent image analyser LAS-4000mini (Fujifilm).

***M. smegmatis* infection of macrophages.** Macrophages were seeded at 1×10^6 cells per well in 12-well tissue culture plates or at 3×10^5 cells per well in 24-well tissue culture plates. Cells were infected with Ms_ppe37 or Ms_vec at an m.o.i. of 20. At this m.o.i., the resulting infection rate was greater than 80 % as estimated in preliminary infection assays from microscopy evaluation of slides stained according to the Kinyon method (Chapin & Lauderdale, 2007). Four hours after infection, gentamicin was added to give a final concentration of 5 μg ml^{-1}. At 6, 24 and 48 h after infection, macrophages were washed and lysed in PBS containing 0.1 % (v/v) Triton X-100. Lysates were plated on Middlebrook 7H10 agar plates containing 25 μg kanamycin ml^{-1} and the number of intracellular bacteria was enumerated.

Assay for lactate dehydrogenase (LDH) release. Culture supernatants were harvested after infection of macrophages with Ms_ppe37 or Ms_vec for 6, 24 or 48 h. LDH activity in the culture supernatants

was assayed with an LDH cytotoxicity detection kit (Takara Bio). The percentage of LDH release was calculated as: percentage release=100 × (experimental LDH release−spontaneous LDH release)/(maximal LDH release−spontaneous LDH release). A value of maximal LDH release was obtained from culture supernatants of macrophages that were lysed with 1 % (v/v) Triton X-100.

Assay for cytokine production. Culture supernatants were harvested after infection of macrophages with Ms_ppe37 or Ms_vec for 24 h. The concentrations of cytokines in the culture supernatants were determined using commercially available ELISA kits for tumour necrosis factor alpha (TNF-α), interleukin 6 (IL-6), IL-1β (eBioscience) and IL-12p70 (Endogen). In some experiments, after infection of macrophages with Ms_ppe37 or Ms_vec for 3, 6, 9, 12 and 18 h, total RNA was extracted with a Nucleospin RNA II kit (Macherey-Nagel). RNA (250 ng) was treated with RNase-free DNase (Promega) and subsequently reverse transcribed into cDNA using a SuperScript VILO cDNA synthesis kit (Invitrogen). cDNAs were diluted tenfold, and a PCR was performed in an equal reaction volume using a KOD-Plus enzyme kit and the following primer pairs: (i) *tnf* gene – 5′-CATGAGCACAGAAAGCATGATCCG-3′ (forward) and 5′-TCTGGGCCATAGAACTGATGAGAG-3′ (reverse), product size 230 bp; (ii) *IL-6* gene – 5′-TTCCTCTCTGCAAGAGACT-3′ (forward) and 5′-TGTATCTCTCTGAAGGACT-3′ (reverse), product size 432 bp; and (iii) *Actb* gene – 5′-TGGAATCCTGTGGCATCCATGAAAC-3′ (forward) and 5′-TAAAACGCAGCTCAGTAACAGTCCG-3′ (reverse), product size 350 bp. Equal volumes of the PCR mixtures were electrophoresed in 1.5 % agarose gel, and DNA bands were visualized with ethidium bromide (2 μg ml^{-1}) staining.

Flow cytometric analysis. Macrophages were harvested after a 24 h infection with Ms_ppe37 or Ms_vec and treated with anti-CD16/CD32 mAb (clone 93; eBioscience) for 10 min. This was followed by a 20 min incubation on ice with one of the following phycoerythrin-conjugated antibodies against: major histocompatibility complex class I (MHC-I; clone 28-14-8), MHC-II (clone M5/114.15.2), B7.1 (CD80 clone 16-10A1), B7.2 (CD86, clone GL1) or CD40 (clone 1C10), or with an isotype control antibody (all from eBioscience). The intensity of each cell-surface marker was analysed on a FACScalibur flow cytometer equipped with CellQuest software (BD Biosciences).

Assay for nuclear factor-kappa B (NF-κB), extracellular signal-regulated kinase (ERK) and p38 phosphorylation. Macrophages were infected with Ms_ppe37 or Ms_vec for 0.5, 1, 2, 4, 6, 7 or 8 h. After infection, macrophages were lysed in buffer containing 10 mM Tris/HCl (pH 6.8), 1 % (v/v) NP-40 and proteinase/phosphatase inhibitor cocktail (Nacalai Tesque). Cell lysates were harvested and subjected to SDS-PAGE. Phosphorylated and unphosphorylated ERK and p38, as well as the phosphorylated p65 subunit of NF-κB, were detected in lots with specific antibodies (Cell Signaling Technology). β-Actin was detected with anti-β-actin antibody (Sigma-Aldrich). Chemiluminescent images were captured with a luminescent image analyser LAS-4000mini. In another experiment, macrophages were pre-treated with 20 or 40 μM U0126 (a MEK1/2 inhibitor; Cell Signaling Technology) or with 10 or 20 μM Calbiochem SB202190 (a p38 inhibitor; EMD Biosciences). On the basis of preliminary experiments, the inhibitors were used at the concentrations required to inhibit ERK and p38 activities. One hour after treatment, the macrophages were infected with Ms_ppe37 or Ms_vec. The culture supernatants were harvested 24 h after infection, and ELISA was performed to determine the concentrations of TNF-α and IL-6.

Statistical analysis. Data were analysed using Student's two-tailed *t*-test. Statistical significance was defined as a P value <0.05. Error bars represent SD.

RESULTS

Ms_ppe37 constitutively expresses *M. tuberculosis* PPE37 protein

In this study, we generated two recombinant *M. smegmatis* strains to investigate the effect of PPE37 on the macrophage response to bacterial infection. The Ms_ppe37 strain was engineered to express a 6His-tagged PPE37 protein from a recombinant pMV261 vector, whilst the Ms_vec strain harboured the vector alone. The pMV261 vector contains the kanamycin resistance gene *aph* for selection of transformed bacteria (Stover *et al.*, 1991). Both Ms_ppe37 and Ms_vec, which were grown in Middlebrook 7H9 medium in the presence of kanamycin, expressed the *aph* gene. However, only Ms_ppe37 was able to express the *ppe37* gene (Fig. 1a). Furthermore, Western blot analysis with anti-penta-His antibody detected a protein band representing PPE37 in the total cell lysate prepared from Ms_ppe37 but not from Ms_vec (Fig. 1b). These results confirmed that the transformation was successful and that *ppe37* gene expression was detectable only in *M. smegmatis* that had been electroporated with the recombinant vector. In addition, Western blot analysis also revealed that a protein band representing PPE37 was detectable in the total cell lysate but not in the culture filtrate fractions prepared from Ms_ppe37 grown in Sauton medium (Fig. 1c). This was not due to the absence of proteins in the culture filtrate fraction, as Coomassie blue staining revealed the presence of many protein bands in both the culture filtrate and the cell lysate fractions. From the result in Fig. 1(c), it could be suggested that PPE37 is not a secretory protein. We also compared the growth kinetics of Ms_ppe37 and Ms_vec in Middlebrook 7H9 medium, as excess production of recombinant protein is known to exert a metabolic burden on recombinant bacteria, sometimes reducing the growth of these cells (Bentley *et al.*, 1990). We observed no marked difference in the growth kinetics (Fig. 1d), indicating that expression of the *ppe37* gene did not influence the growth of Ms_ppe37.

PPE37 does not contribute to the intracellular survival of *M. smegmatis* in macrophages

M. smegmatis is inherently unable to multiply inside macrophages, and the number of intracellular bacteria decreased gradually after infection of macrophages *in vitro*. In order to determine whether PPE37 facilitated the intracellular survival of these bacteria in macrophages, we compared the survival kinetics of Ms_ppe37 and Ms_vec in peritoneal exudate macrophages by conducting a gentamicin protection assay. The results showed no significant difference in the number of bacteria between Ms_ppe37 and Ms_vec up to 48 h after infection (Fig. 2a). Similar results were also observed in bone marrow-derived macrophages (Fig. 2b). These results suggested that the presence of PPE37 was not able to enhance the intracellular survival of *M. smegmatis* in macrophages.

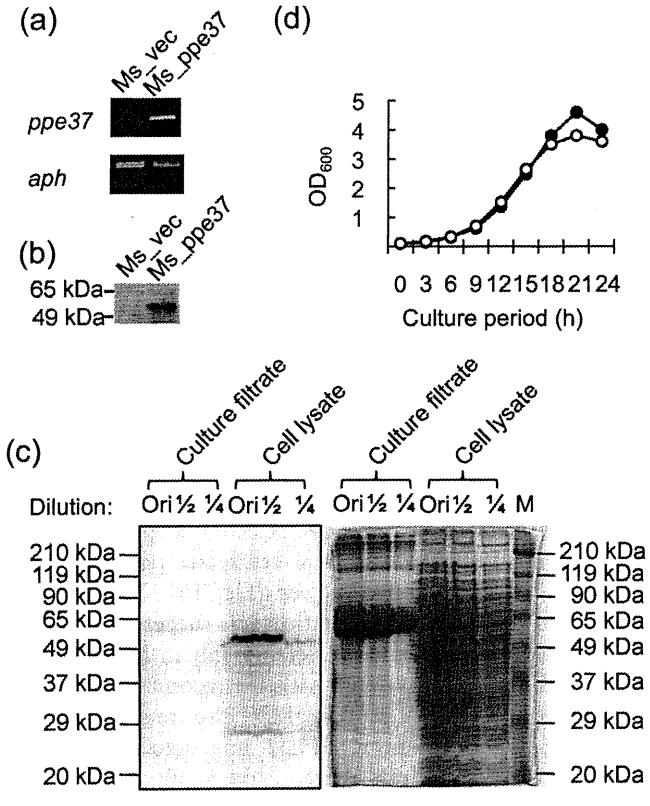

Fig. 1. Expression of *M. tuberculosis* PPE37 by *M. smegmatis* mc^2 155. (a) Ms_ppe37 and Ms_vec were grown at 37 °C in Middlebrook 7H9 liquid medium to an OD_{600} of 0.6–1.0. Total bacterial RNA was isolated and subjected to RT-PCR to detect expression of the *ppe37* and *aph* genes. (b) Lysates were prepared from bacterial cells that were cultured as in (a) and subjected to Western blot analysis to detect His-tagged PPE37 protein using mouse anti-penta-His antibody. (c) Lysate and culture filtrate fractions were prepared from Ms_ppe37 grown at 37 °C in Sauton medium to an OD_{600} of 0.6–1.0. Samples were diluted and subjected to Western blot analysis (left panel) as in (b), as well as to Coomassie blue staining (right panel), after SDS-PAGE. (d) Growth of Ms_ppe37 (○) and Ms_vec (●) at 37 °C in Middlebrook 7H9 liquid medium was monitored by determining OD_{600} at intervals of 3 h. Similar results were obtained in two independent experiments. Ori, Original undiluted sample; 1/2 and 1/4, samples diluted twofold and fourfold, respectively; M, protein marker.

PPE37 does not affect macrophage cell death during infection with *M. smegmatis*

One of the consequences of infecting host cells with *M. tuberculosis* is cell death, with the possibility that *M. tuberculosis* manipulates host-cell death as one of the mechanisms of pathogenicity. Recently, emerging new evidence prompted the proposal of a new model on the interaction between *M. tuberculosis* and its host cell (Behar *et al.*, 2010). This model suggests that, as a pathogenic strategy, virulent *M. tuberculosis* inhibits apoptosis whilst actively inducing necrosis in the infected host cell. The outcome of this strategy is a reduction in the efficiency of

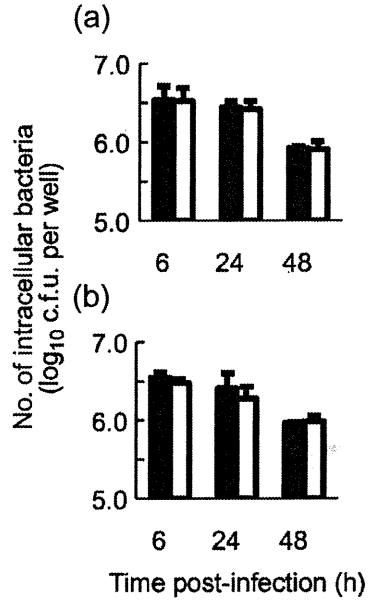

Fig. 2. Intracellular survival of recombinant *M. smegmatis* in macrophages. Peritoneal exudate macrophages (a) or bone marrow-derived macrophages (b) were infected with Ms_ppe37 (white bars) or Ms_vec (black bars) at an m.o.i. of 20. At 6, 24 and 48 h after infection, the macrophages were washed and lysed. Lysates were diluted and plated on Middlebrook 7H10 agar plates containing 25 μg kanamycin ml^{-1} to determine the number of c.f.u. Data are shown as means ± SD of triplicate wells. Similar results were obtained in three independent experiments.

cross-presentation of mycobacterial antigens leading to the impairment in the initiation of T-cell immunity (Behar *et al.*, 2010; Divangahi *et al.*, 2010).

In this experiment, we thus wanted to determine whether PPE37 was able to affect the death of macrophages infected with *M. smegmatis*. Peritoneal exudate macrophages were infected with Ms_ppe37 or Ms_vec, and the amount of LDH released into the culture supernatant (an indicator of cell death) was determined. The result showed that macrophages infected with Ms_ppe37 or Ms_vec released a comparable amount of LDH (Fig. 3). In addition, microscopic examination also revealed no differences in the morphological features of the infected macrophages within the time period of infection (data not shown). Taken together, these results suggested that macrophage cell death was unaffected by PPE37 during infection with *M. smegmatis*.

Ms_ppe37 induces a lower level of pro-inflammatory cytokines in infected macrophages

To deduce the potential role of PPE37 in the virulence of *M. tuberculosis*, we investigated the effect that PPE37 might have on the immune response of infected macrophages. The aspect of the immune response that we examined first was cytokine production. Peritoneal exudate macrophages were

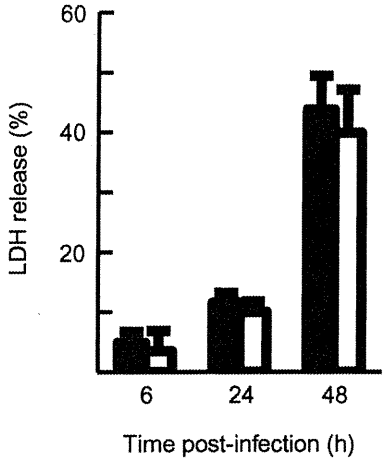

Fig. 3. Assay of cell death in macrophages infected with recombinant *M. smegmatis*. Peritoneal exudate macrophages were infected with Ms_ppe37 (white bars) or Ms_vec (black bars) at an m.o.i. of 20. At 6, 24 and 48 h after infection, culture supernatants were harvested. Release of LDH as a measure of macrophage cell death was estimated by assaying LDH activity in the culture supernatants. Data are shown as means ± SD of triplicate wells. Similar results were obtained in three independent experiments.

infected with Ms_ppe37 or Ms_vec for 24 h, and the concentrations of cytokines in the culture supernatants were determined. Consistent with the cytokine profiles reported elsewhere for macrophages infected with *M. smegmatis* (Lee & Schorey, 2005; Post *et al.*, 2001; Roach & Schorey, 2002), peritoneal exudate macrophages infected with Ms_vec or Ms_ppe37 also produced TNF-α, IL-6, IL12p70 and IL-1β (Fig. 4a–d). However, we discovered that Ms_ppe37 induced a significantly lower level of these cytokines in infected macrophages compared with Ms_vec. We repeated the infection experiment in bone marrow-derived macrophages, and measured the production of TNF-α and IL-6. Similar to infection in peritoneal exudate macrophages, Ms_ppe37 also induced a significantly lower level of TNF-α and IL-6 in the infected bone marrow-derived macrophages compared with Ms_vec (Fig. 4e, f). RT-PCR analyses showed that the expression of TNF-α mRNA in macrophages infected with Ms_ppe37 was delayed compared with the expression in macrophages infected with Ms_vec. The difference in the expression level was observed until 9 h after infection and thereafter became comparable (Fig. 4g). Although expression of IL-6 mRNA occurred much later, from 12 h after infection, the mRNA levels were also lower in macrophages infected with Ms_ppe37 than in macrophages infected with Ms_vec. However, despite the differential cytokine response, flow cytometric analysis revealed no significant differences in the expression levels of MHC-I, MHC-II, CD80, CD86 and CD40 between macrophages infected with Ms_ppe37 and macrophages infected with Ms_vec (Fig. 5). Taken together, these results suggested that PPE37 might possess a functional property that interferes with the pro-inflammatory cytokine production of macrophages infected with *M. smegmatis* but does not affect the expression of surface markers on these macrophages.

PPE37 alters the activation levels of NF-κB, ERK and p38 in macrophages infected with *M. smegmatis*

NF-κB is a major transcription factor responsible for the expression of both TNF-α and IL-6 mRNAs (Collart *et al.*, 1990; Faggioli *et al.*, 2004; Kuprash *et al.*, 1999; Libermann & Baltimore, 1990; Zhang *et al.*, 1994). It has been reported that NF-κB activation is needed to induce the expression of TNF-α and IL-6 mRNAs in macrophages infected with *M. smegmatis* (Gutierrez *et al.*, 2008). In addition, a previous study showed that *M. smegmatis* infection is also able to induce phosphorylation of the NF-κB p65 subunit (Lee & Schorey, 2005). The altered TNF-α and IL-6 mRNA expression shown in Fig. 4(g) therefore raised the possibility that NF-κB activation might be altered in macrophages infected with Ms_ppe37. To clarify this possibility, Western blot analysis was performed and the level of phosphorylated NF-κB p65 subunit in the infected macrophages was assessed. It was observed that Ms_ppe37 induced a relatively lower level of p65 phosphorylation in the infected macrophages compared with Ms_vec (Fig. 6a).

In addition to NF-κB, it has been shown that the expression of TNF-α mRNA in macrophages infected with *M. smegmatis* also requires the activation of p38 and ERK (Lee & Schorey, 2005; Roach *et al.*, 2005). Pharmacological inhibition experiments confirmed the requirement for ERK and p38 activities in the production of TNF-α and IL-6 in macrophages infected with Ms_vec (Fig. 6d, e). These results (Figs 4g and 6d, e) thus led us to investigate whether the activation of these mitogen-activated protein kinases (MAPKs) might also be affected in macrophages infected with Ms_ppe37. Western blot analysis was performed and the levels of phosphorylated ERK and p38 in the infected macrophages were assessed. Fig. 6(b, c) showed that Ms_ppe37 also induced a relatively lower level of ERK and p38 phosphorylation in infected macrophages compared with Ms_vec. The lower transcriptional activation of the TNF-α and IL-6 genes in macrophages infected with Ms_ppe37 therefore might have been due to a lower level of activation of NF-κB, ERK and p38. Taken together, these results further argue for the possibility of PPE37 interfering with the pro-inflammatory cytokine response of macrophages infected with *M. smegmatis*.

DISCUSSION

In the present study, the results suggested the possibility that the *M. tuberculosis* PPE37 protein might interfere with the pro-inflammatory cytokine response in infected macrophages. We found that TNF-α, IL-6, IL-12p70 and IL-1β were produced at significantly lower concentrations by macrophages infected with Ms_ppe37 compared with

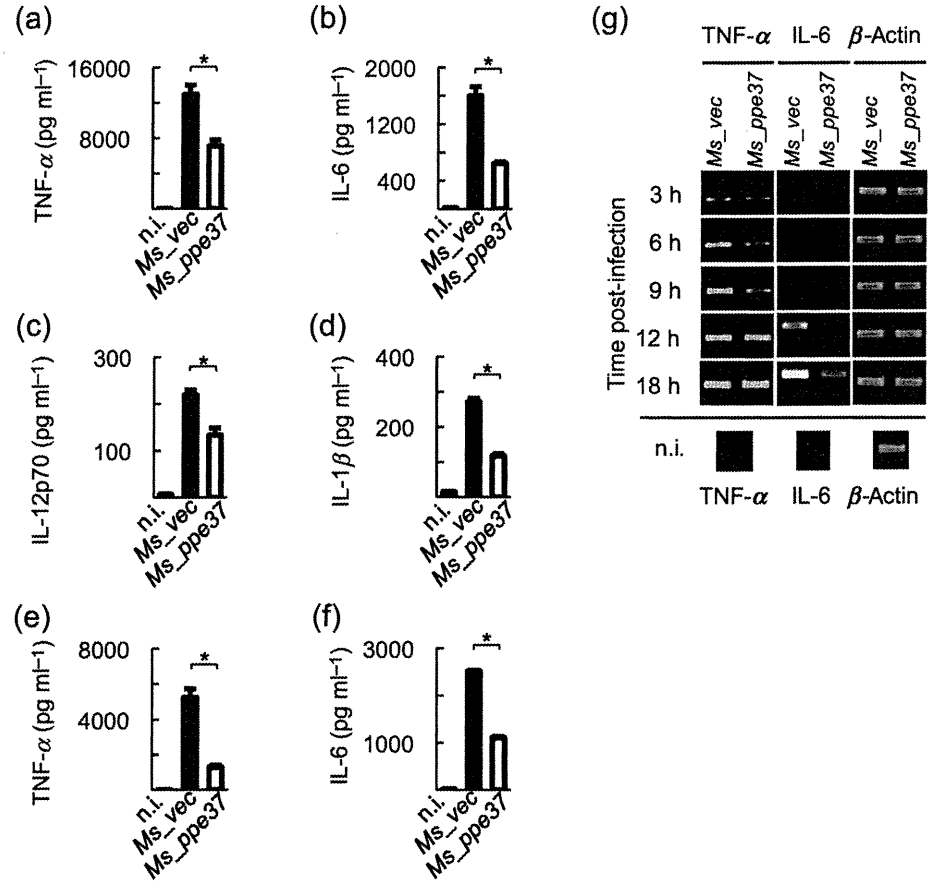

Fig. 4. Production of pro-inflammatory cytokines by macrophages infected with recombinant *M. smegmatis*. Peritoneal exudate macrophages (a–d) or bone marrow-derived macrophages (e, f) were infected with Ms_ppe37 or Ms_vec at an m.o.i. of 20. Culture supernatants were harvested after 24 h of infection and the concentrations of TNF-α (a, e), IL-6 (b, f), IL-12p70 (c) and IL-1β (d) were determined. Data are shown as means ± SD of triplicate wells. *, $P<0.05$ by Student's two-tailed *t*-test. Similar results were obtained in three independent experiments. (g) Peritoneal exudate macrophages were infected with Ms_ppe37 or Ms_vec at an m.o.i. of 20. At 3, 6, 9, 12 and 18 h after infection, macrophages were washed and total RNA was extracted. Equal amounts of total RNA were subjected to RT-PCR in equal reaction volumes. DNA bands were visualized by ethidium bromide staining after equal volumes of PCR mixture had been electrophoresed. Similar results were obtained in two independent experiments. n.i., No infection.

macrophages infected with Ms_vec. The differential cytokine levels were due to lower transcriptional activation of the cytokine genes, which probably resulted from reduced activation of NF-κB, ERK and p38.

To the best of our knowledge, PPE18 is the only other PPE protein that has been reported to exhibit the property of interfering with the pro-inflammatory cytokine response in infected macrophages (Nair *et al.*, 2009). In the study by Nair *et al.* (2009), phorbol myristate acetate-differentiated THP-1 macrophages were infected with either a recombinant *M. smegmatis* strain that expressed PPE18 or a control strain that harboured the vector alone. It was shown that IL-12p40 production was significantly lower in macrophages after infection with the PPE18-expressing strain than after infection with the control strain. Nair *et al.* (2009) concluded that the decrease in the level of IL-12p40 was due to the anti-inflammatory activity of IL-10. A significantly higher production of IL-10 was concurrently found in macrophages after infection with the PPE18-expressing strain. In contrast to our study, we observed very low levels of IL-10 and found no significant difference in the concentration of IL-10 after infection with Ms_vec and Ms_ppe37 (data not shown). Using a purified recombinant protein, Nair *et al.* (2009) showed that PPE18 stimulated the macrophages to secrete IL-10 by binding to Toll-like receptor 2 (TLR2). A consequence of this binding was an early and sustained activation of p38 MAPK, which has been shown to be critical for the induction of IL-10. Similarly, our findings also implied the involvement of MAPKs. However, our study suggests that the mechanism by which PPE37 might interfere with the pro-inflammatory cytokine response in infected macrophages involves reduced transcriptional activation of the

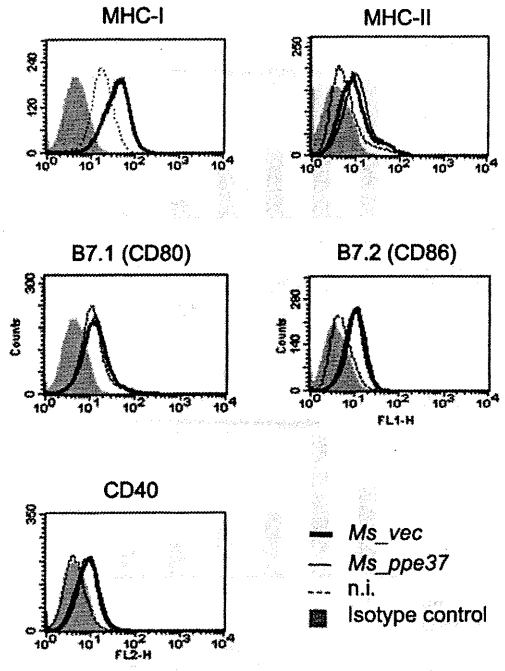

Fig. 5. Expression of cell-surface markers on macrophages infected with recombinant *M. smegmatis*. Peritoneal exudate macrophages were infected with Ms_ppe37 or Ms_vec at an m.o.i. of 20. After 24 h of infection, the macrophages were harvested and the expression levels of MHC-I, MHC-II, CD86, CD80 and CD40 were analysed by flow cytometry. Grey-shaded areas represent the basal fluorescent intensity in macrophages stained with isotype control IgG2a. n.i., No infection.

cytokine genes. This in turn is probably due in part to reduced activation of NF-κB, ERK and p38.

Although both PPE18 and PPE37 exhibit the similar property of interfering with the pro-inflammatory cytokine response in infected macrophages, there appear to be differences in the mechanisms. This is indicated by the discrepancy in the production of IL-10 and also in the pattern of MAPK activation. One of the possible contributing factors may be attributed to a difference in the intrinsic properties of PPE37 and PPE18. Analysis of their amino acid sequences has led to further classification of PPE37 and PPE18 into the PPE-PPW and PPE-SVP subfamilies, respectively (Adindla & Guruprasad, 2003; Gey van Pittius *et al.*, 2006; Gordon *et al.*, 1999). PPE proteins of the subfamily PPE-PPW are characterized by a conserved 44 aa residue region in the C terminus, which comprises highly conserved Gly-Phe-X-Gly-Thr and Pro-X-X-Pro-X-X-Trp sequence motifs (Adindla & Guruprasad, 2003; Gey van Pittius *et al.*, 2006). Members of the PPE-SVP subfamily, on the other hand, contain the motif Gly-X-X-Ser-Val-Pro-X-X-Trp between position 300 and 350 in their amino acid sequence (Gey van Pittius *et al.*, 2006; Gordon *et al.*, 1999). A systematic functional comparison has yet to be made, but these amino acid sequence motifs may confer distinct properties on the respective PPE proteins.

The other factor that may have contributed to the distinct features in the effect of PPE18 and PPE37 on IL-10 production and the pattern of MAPK activation may stem from differences in the responses between mouse peritoneal macrophages and the human monocytic leukaemia cell line THP-1. Differences in MAPK activation are found to differ considerably depending on the cell type used (Rao, 2001). This has led to the assertion that signalling events associated with MAPK activation cannot be extrapolated from one cell type to another (Rao, 2001). In addition to cell type, it has also been reported that the level of cell maturity also affects the activation of MAPK. Indeed, it was shown that, upon infection with *M. tuberculosis*, the kinetics of p38 MAPK activation in human alveolar macrophages was faster than in human blood monocytes (Surewicz *et al.*, 2004).

Our study showed that the phosphorylation levels of ERK, p38 and NF-κB p65 were lower in macrophages infected with Ms_ppe37. This suggests that PPE37 may be interfering with or inhibiting the activation of these molecules. How does PPE37 achieve this, considering that ERK, p38 and NF-κB p65 are three different proteins, each associating with three different signalling pathways? A possible mechanism as to how PPE37 might inhibit or interfere with the activation of ERK, p38 and NF-κB p65 is by inhibiting or interacting with a molecule that is involved in the common activation of these three different proteins. Although the MAPK and NF-κB signalling pathways are distinct, they are not mutually exclusive. For example, they are known to share some common stretches of the signalling pathways when the TLRs are stimulated (Akira *et al.*, 2003). Among the TLRs, TLR2 is most frequently involved in the recognition of various pathogen-associated molecular patterns isolated from *Mycobacterium* spp. (Jo *et al.*, 2007). Therefore, in the innate immune response to *Mycobacterium* spp. including *M. smegmatis*, the activation of MAPKs and NF-κB may occur most commonly through the stimulation of TLR2. In general, the stimulation of most TLRs results in the recruitment of the adaptor protein MyD88 to the receptor complex, where it promotes the subsequent interaction of IL-1R-associated kinase with TNF receptor-associated factor 6 (TRAF6). The signalling pathways from TRAF6 then branch out, with one leading to the MAPK pathway and another to the NF-κB pathway (Akira *et al.*, 2003). This thus makes it very tempting to speculate on the possibility that PPE37 interacts with one of these molecules, including TLR2, that are involved in the common activation of the MAPK and NF-κB signalling pathways. Although the results shown in Fig. 1(c) suggested that PPE37 is not a secretory protein, computational analysis of the amino acid sequence predicted the subcellular localization of PPE37 to be on the bacterial cytoplasmic membrane (Gardy & Brinkman, 2006; http://www.psort.org/psortb/). In line with this, as TLR2 is a cell-surface receptor molecule, it may be more likely to interact with PPE37 than with other molecules in the TLR2 signalling pathways that are involved in the common